THESIS FOR THE DEGREE OF DOCTOR OF PHILOSOPHY

Use of Switchable Carbamate Surfactants for Design of Reversible Colouring of Cotton

ANNA-KARIN HELLSTRÖM

Department of Chemistry and Chemical Engineering

CHALMERS UNIVERSITY OF TECHNOLOGY

Göteborg, Sweden 2019

Use of Switchable Carbamate Surfactants for Design of Reversible Colouring of Cotton

ANNA-KARIN HELLSTRÖM
ISBN: 978-91-7905-216-4

Doktorsavhandling vid Institutionen för kemi och kemiteknik
Chalmers tekniska högskola
Ny serie nr: 4683
ISSN: 0346-718X

Department of Chemistry and Chemical Engineering
Chalmers University of Technology
SE-412 96 Göteborg
Sweden
Telephone +46 (0)31-772 1000

Cover:
Reversible flocculation of colloidal dispersions triggered by switchable anionic carbamate surfactants (reprinted from paper III © with permission from Elsevier).

Printed by Chalmers Reproservice
Göteborg, Sweden 2019

Errata till

Use of switchable carbamate surfactants ... / Anna-Karin Hellström

Ny serie 4683

List of errata

Figure 5: Information missing. Schematic illustration of the Stern model with (solid line) and without (dotted line) electrolyte ions.

Figure 31: Clarification of the reaction:

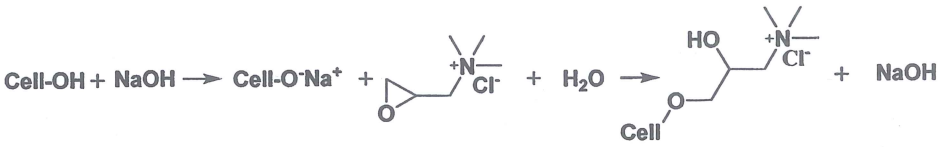

Use of Switchable Carbamate Surfactants for Design of Reversible Colouring of Cotton

ANNA-KARIN HELLSTRÖM
Department of Chemistry and Chemical Engineering
Chalmers University of Technology

ABSTRACT

Circularity of materials is a global need. However, recycling of cotton often requires many steps involving chemical or mechanical treatments. According to the waste hierarchy, reuse is a more environmentally benign approach than recycling, giving extended lifecycles with only limited processing of materials. To facilitate recycling and reuse of cotton, in particular reuse, an important step to meet is the possibility of re-colouring of cotton fabrics.

In this thesis, a new colouring method, with an embedded function for removal of the colour, has been designed. The colouring method is based on pigment nanoparticles, stabilized by a switchable surfactant that enables control of the pigment adsorption at the surface of the fibres through electrostatic interactions. The pigment desorbs from the surface upon exposure to an external trigger, resulting in de-colouring. The switchable surfactant is based on a Y-shaped diamine (denoted Y12-amine), which, by reaction with CO_2 at a pH above the both pKa values of the Y12-ammonium (protonated Y12-amine), forms an anionic Y12-carbamate. The anionic Y12-carbamate reverts to the Y12-amine upon heating, imparted by the cleavable and switchable character of the surfactant.

The work presented in this thesis is divided into three parts. In the first part, the physicochemical properties of the Y12-amine and its carbamates are determined. The formation and stability of the anionic Y12-carbamate were shown to be dependent on pH and temperature. The anionic Y12-carbamate exhibited a higher CMC and less surface activity than the Y12-amine at pH 12. Furthermore, the ion-pair Y12-ammonium-Y12-carbamate, which was formed at neutral pH, exhibited the lowest CMC and the highest surface activity.

In the second part of this work, the anionic sodium Y12-carbamate surfactant was used to disperse and stabilize nanopigments. The effect of pH on the colloidal stability with the anionic Y12-carbamate as surfactant was investigated by measuring particle size and electrophoretic mobility. It was found that the pH value strongly affected the stability of the nanopigments. Moreover, by exposing the pigment dispersion to N_2/heat or CO_2 at pH 12, flocculation and re-dispersion cycles could be achieved without significantly affecting the particle size.

Finally, a hydrophobic pigment stabilized by the anionic Y12-carbamate was used to colour cationised cotton through adsorption. Desorption was triggered by acid hydrolysis of the carbamate groups, generating Y12-ammonium. The mechanical properties of the de-coloured cationised cotton were determined and the maximum tensile stress was found to increase by ~15% and the strain decrease by ~16% compared to cationised cotton. The de-coloured cationised cotton could also be re-coloured. The reversible colouring method on cotton, which is presented in this thesis, demonstrates that pigment-dyeing triggered by the Y12-carbamate surfactant enables reversible colouring of cotton fabric, which can benefit the reuse of cotton.

Keywords: textile colouring, de-colouring, pigment, carbamate, switchable surfactant, cotton

List of publications

I. **Formation, physicochemical and interfacial study of carbamate surfactants**
Anna-Karin Hellström, Hans Oskarsson and Romain Bordes
Journal of Colloid and Interface Science, 2018, ***511****,* 84-91

II. **Carbamate chemistry at interfaces: Practical considerations and challenges of studying amine surfactants**
Anna-Karin Hellström, Lars Nordstierna and Romain Bordes
Journal of Surfactant and Detergents, 2019, ***22****,* 1109-1117

III. **Anionic carbamate surfactants for reversible flocculation of nanoparticles**
Anna-Karin Hellström and Romain Bordes
Journal of Colloid and Interface Science, 2019, ***536****,* 722-727

IV. **Controlling surface charge of pigment to enable reversible cotton colouring**
Anna-Karin Hellström, Lubica Macakova, Marie Syren, Hanna de la Motte and Romain Bordes
Manuscript

Contribution report

I. Main author. Responsible for the experimental work and data analysis, except controlled environment chamber construction and droplet colour analysis.
II. Main author. Responsible for the experimental work and data analysis. NMR measurements were planned, performed and analysed together with co-author.
III. Main author. Responsible for the experimental work and data analysis, except SEM.
IV. Main author. Responsible for the experimental work and data analysis, except SEM, XPS and washing tests.

Table of content

1 Introduction

The fast-fashion textile industry, together with a growing global population and the raising economic welfare, have drastically increased the demand of textiles. The high speed at which fashion trends are moved from catwalk events to everyday stores has led to an increased consumption and disposal of clothing, resulting in disproportionate environmental and social impacts throughout the whole textile supply chain.[1, 2] To break these negative trends, the fashion and textile industry need to integrate sustainable actions into the value chain, and move from the present linear life cycle model, the take-make-waste system, to a circular system in which the textile waste is transformed into new products.[1]

Textile fibres are derived from both synthetic and natural resources, which undergo significant processing before they are converted to textile fabrics. Indeed, the largest environmental impacts from the fashion industry occur during the production phase in processes such as de-sizing, scouring and bleaching as well as in the wet processes (e.g. dyeing, printing and finishing), which also includes high usage of chemicals that may be harmful for the environment.[3] Alwood *et. al.* proposed that the main environmental concerns that the textile industry is facing are greenhouse emissions, over use of water, toxic chemicals, and a high volume of waste.[4] In response to these challenges there is a growing regulatory interest in increasing the reuse and recycling of textiles.[5] This implies changing the mindset and behaviour of consumers to move away from fast fashion trends, and to increase the reuse of textile fabrics. Along with the development of new technologies to facilitate reusability, and if not possible the recycling of textiles. An important advancement in meeting the urgent need to reuse fabric is a procedure for de-colouring and re-colouring of textiles for new uses.

The purpose of this thesis was to develop a new colouring method with an embedded de-colouring function to aid in the reuse of textiles. Instead of colouring with dyes, which usually covalently link to the fabric, colouring with pigment nanoparticles could facilitate de-colouring without significantly damaging the fabric. Furthermore, it opens areas for remediation of the processing water.

In this study the hypothesis was that a stimuli-responsive surfactant, acting as a dispersing agent, could facilitate the reversible adsorption, i.e. adsorption-desorption, of pigments on cotton fabric. The proposed colouring method is based on controlling the electrostatic interactions between the pigment and the cationised

cotton fabric where adsorption would be triggered by electrostatic attraction and desorption by electrostatic repulsion.

Stimuli-responsive surfactants can reversibly and repeatedly change their molecular structure in response to external triggers.[6] The coloured fabric and the stimuli-responsive surfactant are required to withstand washing with a detergent at 40 °C at slightly alkaline pH. Therefore, the core research question is: Can the reversible adsorption of pigment nanoparticles on cotton be achieved by a charge reversal triggered by a stimuli-responsive surfactant? (see Figure 1).

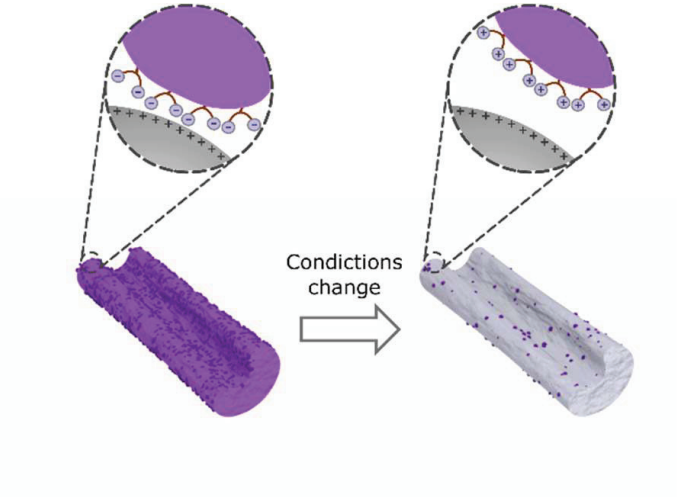

Figure 1. *Hypothetical mechanism of the pigment particle reversible adsorption as mediated by a stimuli-responsive surfactant.*

Carbamate surfactants are interesting candidates for the purpose. They are stable in alkali at 40 °C and they revert to the alkyl amine from which they were made on heating under acidic conditions.

The aims of this thesis were to:

- Find a suitable starting amine, and to understand the physicochemical properties of the amine and its carbamate.
- Study the efficiency of the carbamate surfactant, triggered by CO_2/N_2, to reversibly stabilise and flocculate hydrophobic nanosized pigments.
- Study the reversible adsorption of the pigment on cotton fabrics triggered by the carbamate surfactant.

In **Papers I** and **II**, the physicochemical properties of the amine and the analogous carbamate are described. In **Paper III**, the reversible flocculation of hydrophobic pigment triggered by the carbamate surfactant, is presented and discussed. Finally, in **Paper IV**, the reversible adsorption of the pigment on cationised cotton, triggered by the carbamate surfactant, is described.

2 Surfactants

As mentioned in the introduction, the switchable carbamate surfactant has a leading role in this study. Therefore, in this chapter, the fundamental properties of the surfactant are summarised followed by a short review of stimuli-responsive surfactants and specifically switchable carbamate surfactants.

The IUPAC definition of a surfactant (surface-active agent) is:[7]

"A substance which lowers the surface tension of the medium in which it is dissolved, and/or the interfacial tension with other phases, and, accordingly, is positively adsorbed at the liquid/vapor and/or at other interfaces."

Surfactants are considered as amphiphilic compounds. Amphiphile comes from the Greek with *amphia* meaning "both" and *phil* meaning "love" and is therefore a molecule that has an affinity for two media of different nature e.g. oil and water. Thus, amphiphile possesses both lyophobic (solvent insoluble) and lyophilic segments (solvent soluble). This feature enables the amphiphiles to spontaneous self-assemble to form tightly packed structures at an interface and thereby reduce the free energy of the boundary between two immiscible phases, i.e. reduce surface tension.[8] In water, the segments are usually named hydrophobic (insoluble) and hydrophilic (soluble).

In water at a low concentration, surfactants either exist as free dissolved molecules (unimers) or adsorbed at the interfaces of the aqueous solution. When the concentration increases, more surfactants adsorb at the interfaces and decrease the surface tension up to a specific concentration at which they start to aggregate in the solution and form so-called micelles. The concentration at which they start to form micelles is called the critical micelle concentration (CMC). Above CMC, all further added surfactants form micelles while the unimer concentration remains constant in bulk.[8]

In the micellisation, the major forces that govern self-assembly of surfactants in water are the hydrophobic attractions, which induce the hydrophobic segment to associate, and the ionic or steric repulsion of the hydrophilic segment, which prefers to remain in contact with water (see Figure 2).[9] These two forces act oppositely to each other, mainly in the interfacial region and determine the interfacial area per molecule (effective headgroup area). Hydrophobic forces (attractive) tend to drive towards

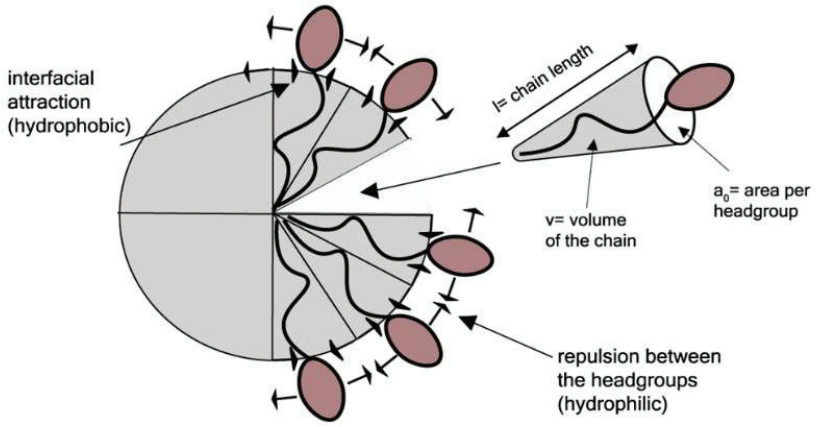

Figure 2. *Illustration of the self-assembly of surfactants into micelles. The interior of the micelles consists of the hydrophobic chains and is in a fluid state. A balance between the attractive hydrophobic forces at the interface and repulsive hydrophilic forces between the headgroups determine the interfacial area per molecule* a_0*. Note, this is only an illustrative image and it does not represent surfactant self-assembly in reality where the hydrophobic chain packing density is even throughout the core. The packing of the hydrophobic chain in the core of the micelle is as disordered as in bulk. Redrawn from ref 9.*

decreasing the interfacial area, while the repulsive forces between the headgroups, tend to do the opposite.

Each surfactant has its own unique CMC, depending on the length and structure of the hydrophobic chain, and the size, polarity and charge of the headgroup. Micelles refer to surfactants that are packed into closed structures and the aggregate shape depends on the structure of the surfactant.

2.1 Stimuli-responsive surfactants

Surfactants that possess more features than surface activity are sometimes called functional surfactants.[8, 10] One class of functional surfactants is stimuli-responsive or switchable surfactants, which are amphiphiles that reversibly and repeatedly change molecular structure by responding to external triggers.[6] As a consequence of the reversibility, the surfactants can alter both interface and bulk solution properties such as surface activity, wettability, viscosity and solubility. This switchable feature is of interest in this research because it could hypothetically enable the reversible pigment colouring of cotton fabric.

An extensive review of stimuli-responsive surfactants was published by Eastoe and co-workers.[6] Typical triggers are pH,[11] UV-light,[12] redox reactions,[13] magnetic field[14] and CO_2.[15] One trigger that has received a lot of attention over the last decade is CO_2 to be used as trigger for pH responsive surfactants. It is well known that CO_2 decreases the pH of an aqueous solution and by purging an inert gas such as N_2 into the solution, CO_2 is removed, and pH increases again. This concept was implemented to pH-responsive surfactants, first by Jessop[15] and later by many others.[6, 15-21] By the simple use of these gases, the surface activity of pH-responsive surfactants can be reversibly altered while avoiding the problem of salt built-up when mineral acids and bases are used.[15, 17, 18, 22-26]

The most studied CO_2-switchable surfactants have a functional group based on alkyl tertiary amine or amidinium that reversibly switch between a protonated and unprotonated state when pH is shifted below and above pKa, i.e. reversible transformation between cationic and non-ionic surfactant.[22] The dissolution of CO_2 in the aqueous solution decreases pH and converts the non-ionic tertiary or amidine amine to a cationic bicarbonate salt.

To the best of our knowledge, there are only a few studies that report CO_2 responsive anionic surfactants; e.g. phenolate and carboxylate salts for the remediation of oil-contaminated sand[27] and potassium dodecyl seleninate surfactant for reversible emulsions.[28]

2.2 Carbamate surfactants

When dissolved in water, CO_2 not only reduces the pH, it may also react with primary and secondary amines to form carbamates.[29, 30] Primary and secondary alkyl amines are known to form an ion-pair composed of alkyl ammonium-alkyl carbamate when exposed to CO_2 (Figure 3 (2)). Most of the early studies on alkyl ammonium- alkyl carbamate formation with focus on self-assembly were conducted by Rudkevich[31] and Weiss[32] and the ion-pairs have been employed as organogelator,[33] for nanocrystal synthesis[34, 35] and in general for controlling self-assembly.[24, 36]

Figure 3 illustrates the strong pH dependency of the reaction of CO_2 with an alkyl amine in an aqueous solution. At a pH well above the pKa, the amino groups is not protonated and the lone pair of electrons on the primary amine reacts with CO_2 and forms an anionic surfactant, i.e. an alkyl carbamate.[36] At a pH around the pKa,

approximately 50% of the amino groups is protonated, and the anionic alkyl carbamate is only partially formed. The resulting product is an ion-pair composed of alkyl ammonium – alkyl carbamate. When the alkyl chain is long, precipitation occurs as the van der Waals interactions promote ion-pair formation, generating a catanionic surfactant, which has low solubility in an aqueous solution.[37] At low pH, well below the pKa, the amino groups is protonated; thus, a cationic surfactant is generated. The ammonium surfactant does not react with CO_2.

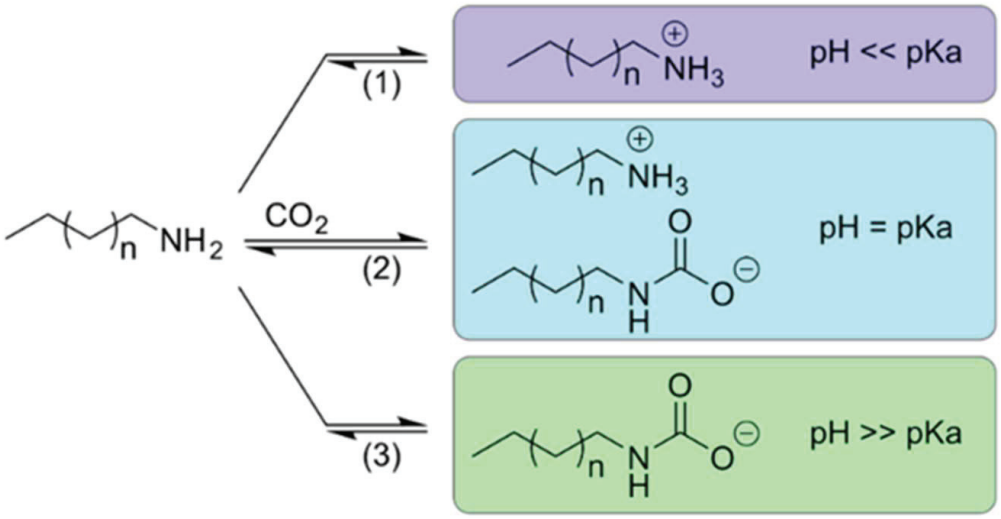

Figure 3. *Reaction of CO_2 with alkylamine at various pH. (1) alkylammonium (cationic surfactant) (2) ion pair of alkylammonium – alkylcarbamate (catanionic surfactant), (3) alkyl-carbamate (anionic surfactant). Reprinted from Paper I © with permission from Elsevier.*

Carbamate formation is reversible and the fatty amine can be regenerated by exposure to N_2, or any other inert gas, and heating.[36]

The parameters that influence the formation and stability of carbamate surfactants are mainly pKa and solubility of the amine.[38] All these parameters are dependent on the structure of the amine. Despite a good understanding of the behaviour of simple alkylamines and their reactivity with CO_2 in water, limited number of studies discuss the relationship between *anionic* carbamate surfactant formation, the molecular structure of the amine used, and the behaviour in solution and at the gas-water interface.[36, 39] Furthermore, the most unique property of switchable carbamate surfactant is that it contains dual functionalities, both being cleavable and

transformable from anionic to cationic surfactant (see Figure 4). This unique property is utilised in this research.

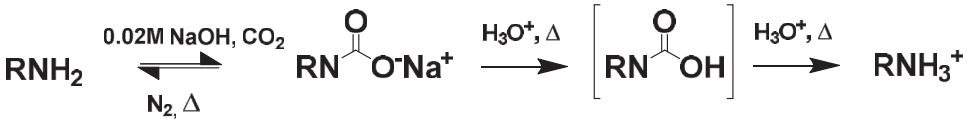

Figure 4. *The unique properties of switchable carbamate surfactants, i.e. dual functionalities as cleavable and transformable from anionic to cationic surfactant.*

3 Theory of colloidal stability

In this study, nanoparticles of pigment have been used for cotton dyeing. Therefore, knowledge of colloidal interactions is essential. This chapter shortly summarises the most important aspects of colloidal chemistry, and how it is applied in colouring cotton.

3.1 Colloidal stability

Hydrophobic particles are inherently unstable, and particles are attracted to each other by van der Waals interactions and eventually coagulate. In practice they can be kinetically stabilised by adsorption of polymers or surfactants. In this research, mainly hydrophobic particles have been studied, and the stability of these particles are quantitatively described by the classical DLVO-theory.[40]

Colloidal stability is governed by the competition between attractive and repulsive forces. The total inter-particle potential energy V_{T} is defined as:

$$V_{\mathrm{T}} = V_{\mathrm{R}} + V_{\mathrm{A}} \qquad (1)$$

where V_R is the repulsive potential energy originating from the repulsions between particles, V_A is the attractive potential energy due to van der Waals attraction.

Attractive forces

Usually, colloidal particles agglomerate due to attractive van der Waals interactions, which originate from the polarizability of the atoms in the particles. A substantial contribution to the attractive interactions is from the dispersion interactions, which is the result of fluctuations in the instantaneous positions of the electrons surrounding the atoms. If one considers two interacting particles in a dispersion, all atoms in the first particles apply a force on the atoms in the second particles and vice versa. By summing up all these pair-wise interparticle attractive forces, the magnitude of the overall interparticle attractions can be assessed and is represented by the Hamaker constant.[41] The effective Hamaker constant will vary depending on the media, surface density and polarizability and it is always positive for identical particles. Importantly, when a layer of surfactants or polymers is adsorbed, on the particle surface, the effective Hamaker constant will be influenced.[42]

The van der Waals interaction energy, V_A, between two identical spherical particles can be defined as:[9]

$$V_{\mathrm{A}}(h) = -(Ar) \,/\, (12h) \quad (h << r) \qquad (2)$$

where h is the particle to particle centre distance, A is the Hamaker constant and r is the radius of the particle.

The total van der Waals attraction force between particles is directly proportional to the size of the particles. The larger the particle size is, the larger the attraction force will be. Furthermore, it is also inversely proportional to the distance between particles.

The attractive forces and Brownian motion will cause particles in a medium to collide with each other and agglomerate over time if no repulsive forces exist to counterbalance the attractive forces. The repulsive forces can either be introduced by an electrostatic double layer as in form of adsorbed ionic surfactants (electrostatic stabilisation) or layers of non-ionic polymers or surfactants covalently linked or physically adsorbed on the particles (steric stabilisation).[8] Finally, a combination of the two exists, which is called electro-steric stabilisation.

Repulsive forces – Electrostatic

Charged particles dispersed in water affect the distribution of dissolved ions in the water and give rise to the so-called electrical double layer as the ions rearrange to screen the surface charge. Several models have been developed to describe the double layer, but in this thesis, only the Stern model will be briefly discussed (more information about the history of the development of the different models of the double layer can be read in reference 43). Stern proposed that the double layer should be divided into two parts.[43, 44]

1) The Stern layer: the ions with an opposite charge to the particle will have an increased concentration close to the surface. This layer of adsorbed ions close to the charged surface is called the Stern-layer.

2) The diffuse layer: counter-ions along with co-ions outside the Stern layer are less adsorbed to the surface and form the diffuse layer.

According to the model, the potential is assumed to change linearly from the particle surface Ψ_0 to the Stern plane Ψ_S and decays to zero in the diffuse layer. The Debye length is referred to as the thickness of the diffuse layer. The thickness of the diffuse

layer can be estimated with the Gouy-Chapman theory where the following assumptions have been made:[9]

- The ions in the solution are assumed to be point charges
- Correlations between the ions in solution are not taken into account
- The surface charge is homogeneous
- The liquid is homogeneous and the dielectric constant, ε_r is not affected by the electric field from the surface

When two charged surfaces approach each other their diffuse layers start to overlap, which gives rise to a repulsive electrostatic interaction. The magnitude of the electrostatic repulsion correlates with the surface potential Ψ_0. The strength of the electrostatic repulsion increases as the magnitude of the surface potential increases. The thickness of the diffuse layer, the Debye length, depends on the electrolyte concentration. The Stern model, with and without electrolyte ions, is schematically shown in Figure 5. Generally, instead of true surface potential, the electrophoretic mobility, or calculated Zeta potential, is used because it is a measurable quantity. The plane of shear is often considered to be at the Stern plane.

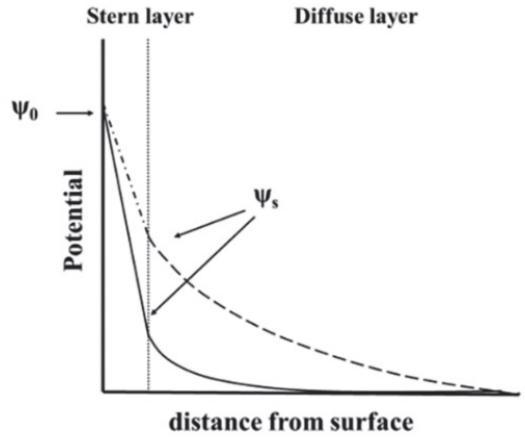

Figure 5. *Schematic illustration of the Stern model with the surface potential as the function of distance from the surface. Ψ_0 is the surface potential and Ψ_S is the potential at the Stern plane. The plane of shear is often considered to be at the Stern plane. Image modified from reference 40.*

Repulsive forces - Steric

In the DLVO theory, only the electrostatic repulsive force is considered, but colloidal stability might be enhanced by other mechanisms such as steric interactions. Steric repulsive forces are governed by adsorbed non-ionic polymers or surfactants on the particles. A monolayer of the polymer or surfactant on the particle surface promotes stability. There are mainly two different theories for steric stabilisation i.e. osmotic repulsion and entropic stabilisation and both are the result of loss in entropy.[40] The osmotic repulsion is a consequence of crowding of polymer chains in the overlapping region, when two particles collide, causing a local increase in osmotic pressure as a result of the disproportion in concentrations of polymer and solvent. The entropic stabilisation is when two opposite polymer chains penetrate each other and compress, which results in a decrease in degrees of freedom of the chains (decrease in configurational entropy).

3.2 The DLVO theory

The DLVO (Derjaguin-Landau-Verwey-Overbeek) theory quantitatively describes the effects of electrostatic repulsive forces and van der Waals attractive forces in the interaction energy and it is the competition between these two forces that determines stability of the colloidal system. The theory assumes that the forces are independent and can be superimposed or added at each interacting distance for two particles. A typical inter-particle potential-distance curve is shown in Figure 6.[40]

The potential energy curve in Figure 6, shows two minima, a primary minimum at a short distance from the surface and a secondary minimum at a larger distance. These two minima are separated by a maximum, i.e. energy barrier. If the particles are close to each other and have passed the energy barrier, the particles will associate irreversibly in the primary minimum. This irreversible association is usually called coagulation. If the particles coagulate in the primary minimum, the particles are strongly attached to each other. If the energy barrier is adequately high, it will prevent particles from coagulating (associate irreversibly) in the primary minimum leading to flocculation (reversible association) in the secondary minimum, where particles are held together by weaker attractive interactions than in the primary minimum.

The main conclusions of DLVO theory are:

- Particles with a large Hamaker constant will display strong attraction
- High surface potential generates higher repulsion between particles and

a more stable colloidal dispersion

- An increase in bulk electrolyte concentration will compress the diffused layer and the apparent surface potential decreases, thus resulting in a decrease of the electrostatic repulsion and stability

A more complex question of particle interactions arises when surfactants cover the surface, since the film of surfactants adsorbed at the surface of the particle will be the dominant factor determining the inter-particle contact. Surfactants are well known to stabilise colloids by adsorbing on the surface, thereby changing the surface properties.[8, 40] In that case, the surfactant layer will be the surface to consider to anticipate the colloidal stability of the system.

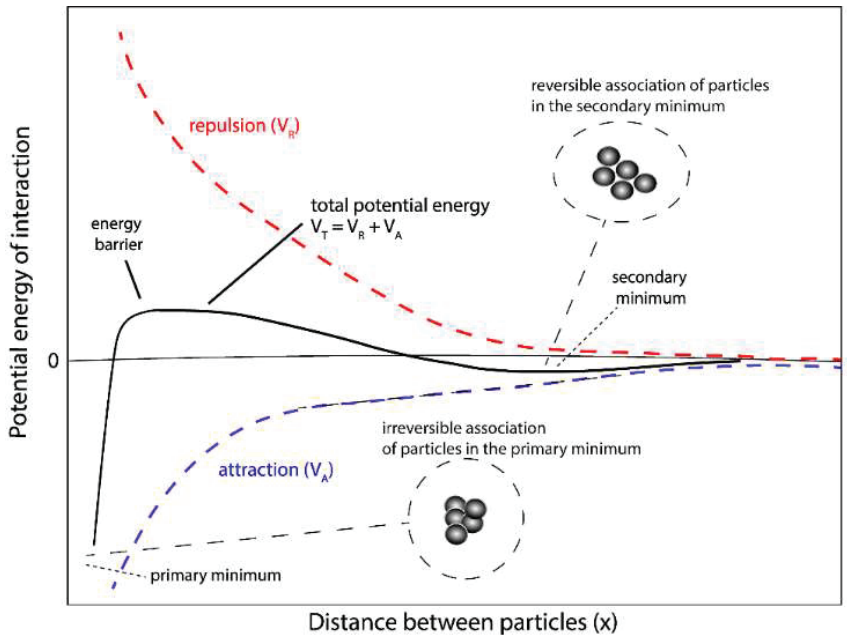

Figure 6. *Image of a typical inter-particle potential curve showing the potential energy of interaction as a function of the distance between particles. The height of the energy barrier indicates how well the particles are stabilised. Particles irreversibly associate (coagulate) in the primary minimum. This means that the particles adhere strongly to each other and are difficult to separate. In the secondary minimum, particles reversibly associate (flocculate) and are loosely attached to each other. Redrawn from reference 40.*

3.3 Reversible flocculation of colloidal dispersions

By choosing the appropriate surfactants and/or surface-active polymers, a stabilised colloidal dispersion can be achieved even for hydrophobic particles in aqueous media, as in the case of the present thesis. Surfactants adsorb readily on hydrophobic and hydrophilic surfaces in aqueous solution. When the surfactants adsorb at a hydrophobic surface, they form a monolayer or self-assemble at the surface under the form of hemimicelles. In aqueous media the hydrophilic part of the surfactant will provide stabilisation and the stability of the repulsive forces will depend on the nature of the polar headgroups. An important aspect of this thesis was to study the reversible flocculation of the pigment nanoparticles. This could hypothetically be achieved by stimuli-responsive surfactants, or as in this thesis carbamate surfactants.

Stimuli-responsive surfactants and polymers have been used to reversibly switch colloidal dispersions between a dispersed and flocculated state. Bijlard *et. al.* have written a comprehensive review of functional colloidal stabilisation where the surfactant design has been tuned for specific applications.[45] To switch between a dispersed and flocculated state, mainly stimuli-responsive surfactants that respond to changes in pH, and are triggered by CO_2 have been reported. A few studies have also been published on redox,[46] magnetic,[47] light-redox,[48] and thermo-responsive[49] surfactants/polymers. As aforementioned, Jessop and co-workers developed the first CO_2-responsive switchable surfactant based on guanidine,[15] and Zang *et al*. later employed this functionality to flocculate and re-disperse latexes.[18] Since then, the interest in the reversible flocculation of colloidal dispersions with CO_2-responsive functionality groups has steadily increased.[16, 18, 19, 50]

In all these studies, CO_2 has been used as a pH regulator, and only a limited number of studies have reported CO_2 to be used as covalently linked to a CO_2-responsive *surfactant* to reversibly flocculate *anionic* colloidal dispersions.

4 Surface properties of cotton fibres and pigments

When colouring textile, both the properties of pigment dispersions and textile fibres are important. In this section, the most essential properties of the pigments and textiles used in this thesis are described, in order to provide the reader with knowledge to understand the colouring method with the embedded de-colouring function.

4.1 Cotton

Cotton fibres consist of 82-96% cellulose and are one of the purest natural forms of cellulose.[51] All-natural fibres, not only cotton, are composed of macromolecules resulting from the polymerisation of smaller entities. In cotton, the macromolecule is cellulose, which is composed of thousands of repeating glucose monomers. The cellulose macromolecules are straight oriented, parallel in a longitudinal direction with the fibre axis, which enables them to self-assemble by hydrogen bonds and van der Waals forces. This regular arrangement of molecules give rise to the crystalline portions in the fibre. Usually, the naturally occurring cellulose fibres contain a 60-70% crystalline structure.[52] Through chemical treatment, the crystallinity can be altered, which is generally desired as a high crystalline structure results in higher stiffness and strength. Decreasing the crystallinity of the structure results in lower strength because the less ordered regions are composed of molecules that are not aligned with the fibre axis. This means that shearing occurs when an axial force is applied on the fibre. On the other hand, the elongation would increase since the molecular chains in the less ordered region would extend in the direction of the fibre axis.

Cotton fibres have a staple length of between 9 – 60 mm and a fibrillar structure that assumes a flat convoluted ribbon like shape with a cross-section which has a kidney-like shape. Cotton contains up to 10 000 monomers of glucose per cellulose macromolecule, in a spiral and linear form within the fibre. However, due to its natural origin, the fibre can vary in length and orientation, yielding different internal structure and surface properties, which can have an impact on the fibre strength, water absorption, dyeing etc.[53] If many cotton fibres are spun, a yarn is formed, and as expected, with increasing yarn twists, the yarn compactness increases. A weave consists of two components that are interlacing at right angles; warp and weft. In this thesis, plain weave cotton fabric has been used, which has an interlacing pattern of weft yarn having a one-up-one-down pattern on the warp yarn. The warp and weft count may increase after specific chemical treatments or washing due to shrinkage.

4.1.1 Cationisation of Cotton

When immersed in water, cotton possesses a slightly negative charge in neutral and alkali aqueous solutions due to the presence, of carboxyl groups.[54] Most commercial reactive dyes consist of anionic dyes, which have low affinity for cotton due to the electrostatic repulsion. In conventional dyeing, high concentration of electrolytes and excess concentration of dyes are required to enable the adsorption of dyes. This leads to environmental problems related to high salt and dyes concentration in the wastewater treatment systems.[55] To overcome these problems, the cationisation of cotton has been extensively researched over the last decades since the first attempt made by Rupin, using glycidyltrimethylammonium chloride.[56] The dyeing process of cationised cotton has been shown to consume fewer chemicals, water and energy compared to the conventual dyeing process of untreated cotton fabric, by promoting electrostatic attraction between dye and fibre.[57]

Furthermore, COD (chemical oxygen demand) of the dye waste stream from cationised cotton is lower than untreated cotton. Therefore, related to these parameters, the dyeing process of cationised cotton is more sustainable but the chemicals used, are toxic to human health.[58] Furthermore, the mechanical properties such as tensile strength can be affected by the pre-treatment of the cotton fabric.[59] Therefore, more research is needed to find a suitable cationising agent with a better toxicity and environmental profile.[60] However, the focus in this thesis has not been to optimise the cationisation, and so, a slightly modified method for the cationisation of cotton based on 2,3-epoxypropyl trimethylammonium chloride (EPTAC) has been used.[61]

4.2 Dyes and Pigments

Dyeing is the result of applying dyes or pigment on textile fabric to achieve the desired colour. When using pigment, the process for colouring textile is either referred to pigmentation or pigment dyeing in the literature. For the sake of clarity, dyeing is referred to as pigment dyeing in this thesis.

Dyes and pigments possess colour because of their chromophores that selectively absorb a certain wavelength of light in the visible spectrum (400-700 nm). With the presence of all the wavelength of visible light, the light appears “white” to the human eye. When a wavelength is absorbed, the eye perceives the remaining wavelengths as the “complementary colour”. The absorption of visible light by the dye or pigment is

promoted by electron transitions. The electron is moved from a lower energy state to a higher energy state and the energy of the absorbed light is equal to the energy difference between the highest and lowest energy states. Therefore, the wavelength of light required to excite an electron from the ground to excited state is specific for each compound. By altering the chemical structure of the compound, the wavelength of the absorbed light can be changed and therefore, the colour of the dye or pigment will be different.[53]

Dyes entails mainly molecules that in most cases colour textiles by the chemical linkage to the fibre while pigments consist of particles that physically adsorb at the surface. However, there are many different types of dyes and all of them do not covalently link to the fibre, but it will not be discussed in this thesis. In this thesis, pigment dyeing for colouring has been used since they physically adsorb on the surface rather than covalently link, which hypothetically could facilitate the de-colouring process. The adsorption of pigments at the surface of fibres to ensue colour is complex because the interaction between pigment and surface depends on the cotton fabric and surface modification used. Furthermore, it also depends on the pigment used.

4.3 Nanosized pigments

Pigments can be defined as:

"substances consisting of particles which impart colour through selective absorption and scattering of light"[62]

Both organic and inorganic pigments exist but, in this thesis, only organic pigments have been studied. Therefore, only organic pigments will be briefly discussed below. Organic pigments are dominantly synthesized by precipitation and are build-up of different crystal structures. They are usually insoluble in aqueous media but can be modified or surface treated to enhance dispersibility in water. Due to their large particle size they will not easily diffuse into the matrix of the fibre, but rather adsorb at the surface of the fibre.[63] Cotton fabric is mostly coloured with reactive dyes, which covalently link to the cellulose, because of the bright colours, excellent fastness and ease of application. However, the benefit of pigment over reactive dyes is that no rinse-off is required to remove excess pigment from fabric, due to the binder that is used to lock the pigment on the fabric surface in the traditional pigment dyeing process. Moreover, the recycling of pigments is easier than dyes due to their larger size and possibility to flocculate, and by that be separated.

The drawbacks of pigment-dyeing are, however, lower colour strength and poor rubbing fastness.[64] One important characteristic of the pigment-dyeing of textile fabrics is that the particle size should be monodispersed with narrow range

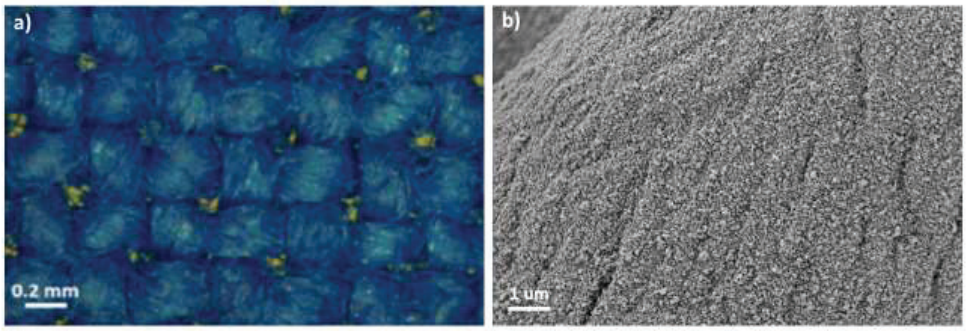

Figure 7. *Cationised cotton coloured with Heliogen Blue 15:3.* ***(a)*** *optical micrograph* ***(b)*** *Scanning Electron Microscopy micrograph.*

distribution to ensure the homogeneous adsorption of the pigment on the cotton surface and thus homogeneous colouring (see Figure 7).[65] In this study the following pigment have been used; pigment Violet PV23, Heliogen Blue 15:3 and Yellow 74.

4.4 Reversible adsorption of pigment on cationised cotton

Adsorption of pigment nanoparticles on cationised cotton could be considered as adsorption of nanoparticles on a solid surface and is mainly driven by electrostatic and van der Waals interactions.

The energy of adsorption of a pigment on a textile can be described as the work of adhesion, which is defined as:

$$W_A = \gamma_{(LC)} + \gamma_{(LP)} - \gamma_{(PC)} \qquad (3)$$

where γ is surface free energy, with L denoting the liquid, P the particle and C the cationised cotton.[40]

The pigment is moved from a low energy level when attached to the textile surface to a higher energy level when desorbed and dispersed in the aqueous medium. Therefore, desorption of pigment from a textile surface requires external energy

To obtain desorption, the work of adhesion has to be reduced. Addition of surfactant reduces $\gamma_{(LP)} + \gamma_{(LC)}$, thus facilitating desorption of the nanoparticles. Finally, desorption of nanoparticles occurs when the sum of the free energies of the particle-water interface and the cationic cotton-water interface is lower than the free energy of the particle-cationic cotton interface:

$$\gamma_{(PC)} > (\gamma_{(LP)} + \gamma_{(LC)}) \qquad (4)$$

In this study, the hypothesis was that the carbamate surfactant would decrease the work of adhesion by inducing charge reversal of the pigment.[66, 67]

The challenges that have to be overcome are:

1) High affinity of the pigment to the textile surface to withstand desorption during washing.
2) Upon demand, breaking the affinity of the pigment on the cationised cotton fabric to facilitate de-colouring of the pigment.

5 Methods for Analysis

In this section, the most important techniques which were used in this thesis are summarised. To understand the reversible colouring of textile of the nanoparticles of pigment stabilised by Y12-carbamate surfactant, the surface properties of the surfactant species were investigated. The surfactants properties were investigated by the pendant drop technique and NMR spectroscopy in order to understand the formation of carbamate from the Y12-amine. The colloidal stability of the pigment stabilised by anionic Y12-carbamate surfactant was investigated by dynamic light scattering and electrophoretic mobility measurements. Finally, the properties of coloured and de-coloured cotton fabrics were investigated by colourimetry and tensile strength measurements.

5.1 Surface tension measurements under a controlled atmosphere

In this research, the pendant drop technique has been used to determine the surfactant's CMC. This was done by measuring surface tension as a function of the concentration of the surfactant. Furthermore, this technique was used to investigate whether the formation of carbamate occurred at the gas-water interface (**Paper I** and **II**). To control the gas atmosphere, the drop was suspended inside a 3D-printed sealed chamber. A scheme of the chamber is shown in Figure 8.

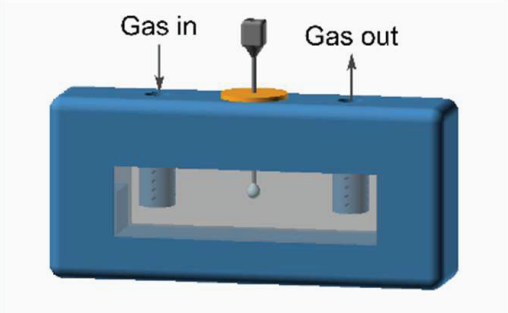

Figure 8. *Display of the 3D printed chamber for the interfacial study. Reprinted from Paper I © with permission from Elsevier.*

The pendant drop technique was used to determine the surface tension or interfacial tension between two different phases. The method is suitable for measurements of surface or interfacial tension between gas-liquid or liquid-liquid interfaces. A drop is suspended in a liquid or gas where the shape of the drop depends on the balance between gravity and surface forces. Surface tension or interfacial tension is determined by analysing the shape of the drop. This energy is calculated by iterative fitting of the contour of the drop with the Young-Laplace equation. The Young-Laplace equation is related to interfacial pressure and radii of curvature (R_1 and R_2) of the drop.

$$\Delta P = \gamma \left(\frac{1}{R_1} + \frac{1}{R_2} \right) \qquad (5)$$

where, ΔP is interfacial pressure difference, γ is the interfacial tension and R_1, R_2 is the radii of curvature of the droplet.[68]

In this research, when the dynamic surface tension at different gas-water interfaces was studied, the atmosphere of the chamber was controlled by flowing CO_2 and N_2 using a mass flow controller system. An example of dynamic surface tension variation of an aqueous drop of octylamine (28.9 mM) during the exposure of CO_2, which can be seen in Figure 9.

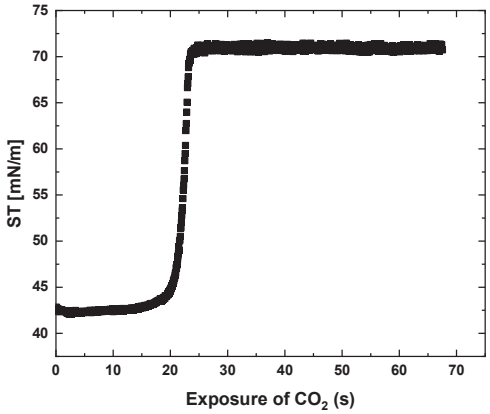

Figure 9. *Example of the dynamic surface tension response of octylamine (28.9 mM) in 0.1 M borate buffer solution at pH 12 during CO_2 exposure.*

CMC was determined from a plot of surface tension versus log surfactant concentration. The surface tension decreases with increasing surfactant concentration until a plateau is reached. CMC is determined at the inflection point (Figure 10). Above CMC, the surface tension is virtually constant.

The adsorption at the interface is related to the surface tension through Gibbs´ adsorption isotherm.

$$\Gamma = -\frac{1}{n\mathrm{R}T} \frac{\delta\gamma}{\delta \ln C} \qquad (6)$$

where Γ is the surfactant surface concentration (mmol m^{-2}), γ is the surface tension (mN m^{-1}), T temperature in Kelvin and R=8.31 (J mol^{-1} K^{-1}) is the idel gas constant, C is the surfactant concentration and n (Gibbs pre-factor) is the number of species at the interface. The Gibbs pre-factor, n has a value of 1 for non-ionic surfactant and larger for ionic surfactants and this will be further discussed in section *"Results and Discussion"*. Surfactant adsorption is determined by the slope of the plot of surface tension versus the logarithm of the concentration. The adsorbed amount of surfactant

is inversely proportional to the cross-sectional area per adsorbed molecule if the adsorbed layer is a monolayer.

$$A = \frac{10^{23}}{N_A \Gamma} \qquad (7)$$

where N_A=6.022 10^{23} mol^{-1} (the Avogadro number), and A the area per molecule in $Å^2$.[69]

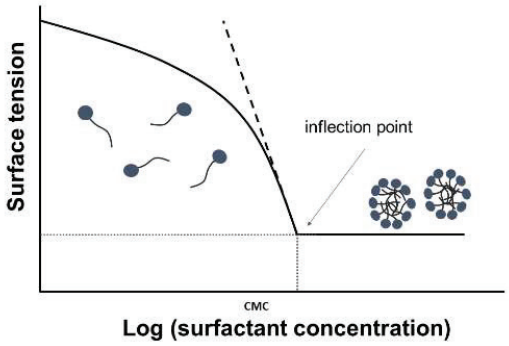

Figure 10. *Surface tension versus the logarithm of surfactant concentration. Critical micelle concentration (CMC) is determined at the inflection point, and the surface tension at the plateau is marked in the figure.*

However, surface tension measurements are highly sensitive to the presence of other molecules as for example surface active impurities, which can provide inaccurate values. Furthermore, the presence of electrolyte in bulk increases surface tension because the electrolyte does not have an affinity for the surface and accumulate in the bulk.[8] Other factors that have been questioned is that the linear region of the surface tension versus log concentration plot prior to the CMC correspond to a saturated interface for *ionic* surfactants. Do the ionic surfactants saturate the interface before forming micelles in the bulk? Theoretically, the adsorption at the interface might not be favoured for ionic surfactants with large headgroups. On the other hand, for non-ionic and mono-ionic surfactants below CMC, Gibbs isotherm model has shown to be in agreement with experiments done by neutron reflectivity.[70] Despite, the questioning of using Gibbs model, it remains a simple and practical method to determine amount adsorbed surfactant at the air-water interface for concentrations below the CMC.

5.2 Nuclear Magnetic Resonance Spectroscopy

Nuclear magnetic resonance, NMR, spectroscopy has been used, in this research, to monitor carbamate formation and determine CMC. Nuclear magnetic resonance is a phenomenon which occurs when a nucleus in a magnetic field absorbs and re-emits electromagnetic radiation. The nucleus of a certain atom is immersed in a static

magnetic field and exposed to a second, oscillating magnetic field. Only nuclei possessing a property called ½ spin, as ^{1}H and ^{13}C will experience this phenomenon. The electron density around each nucleus in each molecule varies depending on the composition and bonding in the molecules. Therefore, the different nuclei are surrounded by different electronic environments and the effective field at each nucleus will vary. This is called chemical shift and will result in different NMR signals for different kinds of nuclei. From these NMR signals, structural information about the molecules can be derived.[71]

In **Paper II**, CMC was determined by ^{1}H-NMR. During micellisation, surfactant changes its environment and as a consequence chemical shifts also change. By monitoring the change in the chemical shift of the terminal CH_3 of the alkyl chain signal in the surfactant as a function of surfactant concentration, CMC can be determined. The CH_3-signal is independent of the amount surfactant present as unimers in the solution until CMC is reached. Above CMC, when the surfactant starts to aggregate, the signal shifts downfield linearly with the inverse of surfactant concentration. Below CMC, the unimers are free in solution whereas above CMC, the observed resonance signal moves downfield due to the equilibrium distribution of surfactant present as micelles and unimers in the solution. An illustration of the shift in position of the CH_3 peak is shown in Figure 11.

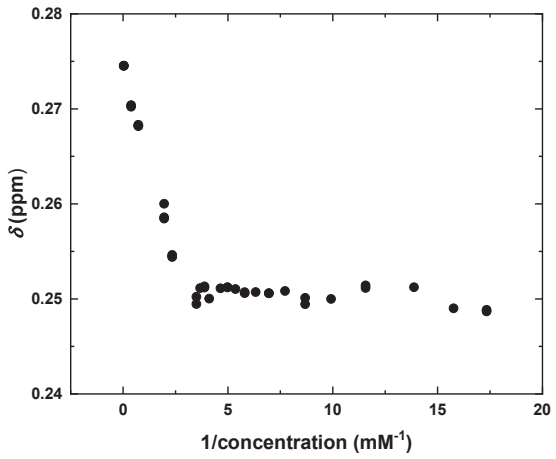

Figure 11. *Illustrated figure of the move downfield in a chemical shift in ^{1}H-NMR versus the inverse of the surfactant concentration for the determination of CMC (Y12-amine). Reprinted from paper II © with permission from Wiley.*

5.3 Streaming Potential

To study the formation of sodium Y12-carbamate at the water-solid interface, the streaming potential as a function of the exposure time of CO_2 was monitored **(Paper III)**. When a pressure is applied to an aqueous medium in a capillary, with charged particles adsorbed at the surface, the mobile counter-ions in the double layer will be displaced and carried toward one end. The accumulation of the ions will build up an electrical field and induce a current to flow in the opposite direction. When a steady

state is reached, the resulting potential difference between the ends of the capillary is measured. This potential difference is called streaming potential. In this thesis, a particle charge detector that consists of a plastic measuring cell with a displacement piston has been used. The gap between the cell wall and the piston is well defined and the suspension of particles is filled in the gap. During measurement, the piston is oscillating and creates an intense flow, which forces the suspension to move and stream through the gap along the cell wall. Some of the particles adsorb at the cell wall and do not follow the force flow within the gap and, therefore, become polarized according to the distortion of the diffuse double layer during the piston movements.[72] In practice not all the particles are adsorbed at the cell wall so the values reported for the streaming potential is not absolute but relative. An example is shown in Figure 12.

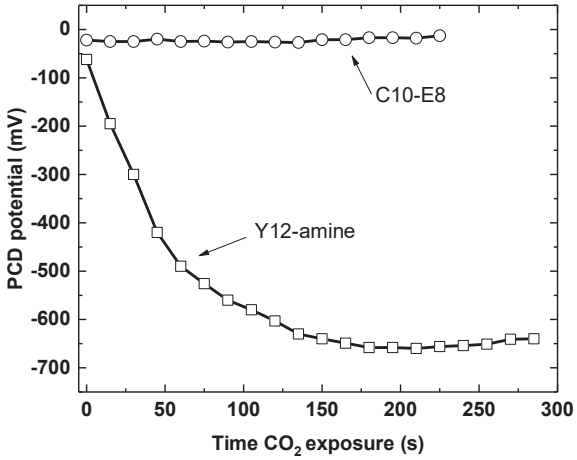

Figure 12. *PCD potential measurements versus time of CO_2 exposure of 0.1 w/w% hydrophobised silica with 19.3 mM Y12-amine at pH 12. A non-CO_2-responsive surfactant (C10-E8 (19.3 mM)) is used as a reference. The values presented in the graph are a mean value of three independent measurements. PCD measures a potential that relates to the streaming potential, but it does not give an absolute value. Reprinted from Paper II ©2019 with permission from Elsevier.*

5.4 Electrophoretic Mobility

To study the electrostatic stabilisation of the pigment dispersions, electrophoretic mobility was determined (**Paper III**). In an electric field, charged particles and the counter-ions surrounding the particles will move through the medium following the line of the field. Electrophoretic mobility U_E, is determined by the velocity of the particle, which can be measured, and the electrical field;

$$U_E = \frac{v}{E} \qquad (8)$$

where v (m^2 s^{-1}) is the velocity and E (V^{-1}) is the applied electric field. The electrophoretic mobility is most often determined by the laser doppler electrophoresis technique. This technique is based on light scattering, where the oriented motion of particles in an electrical field induces a shift in the frequency of the scattered light. The scattered light from the migrating particles is combined with the reference beam to create variations in the intensity from where the velocity can be calculated. In this study, the electrophoretic mobility has been determined by phase analysis light scattering (PALS) rather than the doppler frequency shift. The principle of PALS is that instead of observing the frequency change of the scattered light, it relies on a shift of the phase of the light. The phase shift of the scattered light is proportional to the velocity. This phase shift is measured by comparing the phase of the scattered light of the particle with the phase of a reference beam.[73]

When calculating the Zeta potential from electrophoretic mobility measurements, in this thesis, Henry's equation has been used by the instrument:

$$U_E = \frac{2\epsilon\zeta\ (\kappa r)}{3\eta} \qquad (9)$$

where ϵ is the dielectric constant, η is the viscosity, ζ is the Zeta-potential, $f(\kappa r)$ is Henry's function and varies from 1 to 1.5 as κr varies from 0 to infinity. κ is the Debye-Huckel parameter and r is the radius of the particle. Electrophoretic determination of Zeta potential is most commonly performed in an aqueous medium and moderate electrolyte concentration. $f(\kappa r)$ is in this case maximum and about 1.5 and is referred to as the Smoluchowski approximation. This is valid when the double layer is smaller than the radius of the particle as in the present case.

5.5 Dynamic light scattering

Dynamic light scattering was used to determine the mean particle size and polydispersity of the pigment nanoparticles. The method was useful to monitor the reversible flocculation of the pigment dispersion (**Paper III**).

Dynamic light scattering measures the velocity of macromolecules or particles in Brownian motion. The particles in Brownian motion cause laser light to be scattered, and the particle size can be determined by the intensity, the frequency shift and angular distribution of the scattered light. The Brownian motion originated from the movement of the particles cause a time-dependent fluctuation of the scattering where the fluctuation is correlated to the diffusion rate of the particles. From the diffusion rate, the hydrodynamic diameter can be calculated by using the Stokes-Einstein relationship.

$$D = \frac{k_B T}{3\pi\eta d} \qquad (10)$$

where η is the viscosity, k_B is the Boltzmann's constant, T is the absolute temperature and d is the hydrodynamic diameter.[74]

5.6 Tensile testing

Tensile testing is used to determine a fabric or a single fibre strength (stress) and extension (strain) (**Paper IV**). Strength and extension depend on the internal structure and chemical composition of the fibre. A high crystalline fibre has higher strength and lower extension compared to a fibre with a low crystallinity. The reason is that in a fibre with higher crystallinity, the polymer chains are more stretched compared to a fibre with low crystallinity (more amorphous regions) which consists of less oriented fibres.

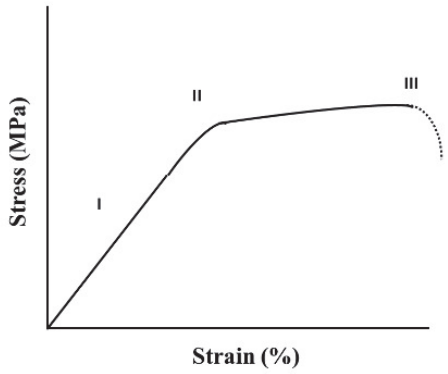

Figure 13. *Illustration of a typical stress-strain curve.*

The relationship between the stress and strain of a fabric or fibre is unique for each material and a typical curve of textile is shown in Figure 13. In region (I), there is a linear relationship between stress and strain, meaning that the extension is reversible when the load is removed. At (II), the fibres are completely stretched and the contact points between the fibres starts to break. This point is called the yield point and the reversibility is lost. At (III), all the fibres have completely broken, and the point is called extension to break and breaking strength.[52]

5.7 Colourimetry

Colourimetry is the science of quantitatively measuring colour by a numerical system and, in this research, it has been used to determine the colour strength of the fabrics **(Paper IV)**. Two colours can appear the same to the human eye but might be slightly different when determined with a colour measurement instrument. The colour is expressed by a three-dimensional (L*a*b*) coordinate system, which was established by the Commission Internationale de l'Eclairage (CIE). L*-value expresses the lightness from black (L=0) to white (L=100), the colour values a* and b*, are neutral grey values at a*=0 and b*=0. a*-value represents green to red component, where green is negative and red is positive. b*-value represents blue-yellow where blue is in the negative direction and yellow in the positive direction. The total difference ΔE is always positive and the equation is shown below:[75]

$$\Delta E = \sqrt{(L_2^* - L_1^*)^2 + (a_2^* - a_1^*)^2 + (b_2^* - b_1^*)^2} \qquad (11)$$

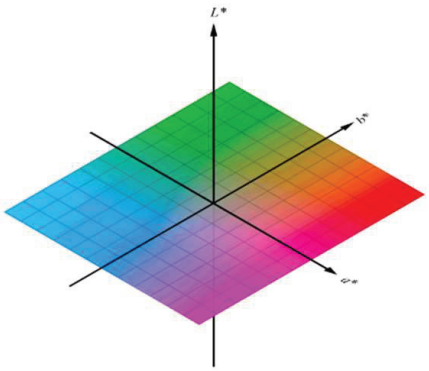

Figure 14. *Colour schematics illustrating the a* and b* values. L* is the z-direction. Under Creative Commons license. Retrieved from Wikipedia.*

6 Results and Discussion

This chapter is divided into three parts and summarizes the key findings of the research presented in the appended papers. Before the ability of pigment nanoparticles to reversibly colour cotton fabric could be investigated, the self-assembly of sodium Y12-carbamate had to be understood. In addition, the efficiency of Y12-carbamate to act as a dispersing agent and its switchable character had to be investigated.

In the first part of this section, the Y12-amine and the corresponding carbamate´s physicochemical properties are presented along with a discussion about the essential parameters for formation of the carbamate species (**Papers I and II**) (6.1). In the second part, the efficiency of the Y12-carbamate surfactant to act as a dispersing agent for the pigment nanoparticles and its switchable character are discussed (**Paper III**) (6.2). Finally, the pigment nanoparticles, stabilized by Y12-carbamate were used to reversibly colour cotton fabric (**Paper IV**) (6.3). Formation, self-assembly and interfacial properties of the carbamate surfactant (Papers I and II)

6.1 Formation, self-assembly and interfacial properties of the carbamate surfactant (Papers I and II)

6.1.1 Bulk behaviour

Dissolution of CO_2 in the presence of a non-self-assembling amine (TETA) and of a self-assembling amine (Y12-amine)

Prior to the study of the amine-based surfactants, it was important to evaluate the dissolution of CO_2 without the presence of a self-assembling amine. For this purpose, triethylene triamine (TETA), which does not contain a hydrophobic segment necessary for micellization, was used.

CO_2 is a stable neutral triatomic molecule that not only reacts with primary and secondary amines to form carbamates, but also dissolves in aqueous media.[76] The solubility of CO_2 in water is low and depend on the pressure and the temperature.[77] However, dissolving CO_2 in aqueous media decreases the pH due to the dissociation of hydrated CO_2. As already discussed, anionic carbamates can only be formed at pH above the pKa of the alkyl ammonium species, therefore, in this thesis, dissolving CO_2 in aqueous solutions containing sodium hydroxide had to be understood. After

the mass transfer of CO_2 (g) into aqueous sodium hydroxide amine solutions, CO_2 can react with either HO^- or with the amine. Rate constants based on non-self-assembling amines are reported in the literature to be of the same magnitude as the reaction of CO_2 with HO^-.[78]

In Figure 15, the decrease in pH over the time, when the surface of the aqueous solution was exposed to a flow of CO_2 (100 ml/min) of three different samples, is shown. The samples consisted of 0.02 M NaOH without amine, with a non-self-assembling amine, TETA, and with a self-assembling amine, Y12-amine. During the exposure of CO_2 to 0.02 M NaOH aqueous solution without the presence of an amine gave a pH decrease from 12 to 6 within ~200 seconds. When the solution consisted of a non-self-assembling amine, TETA, the pH decrease was lower in rate and

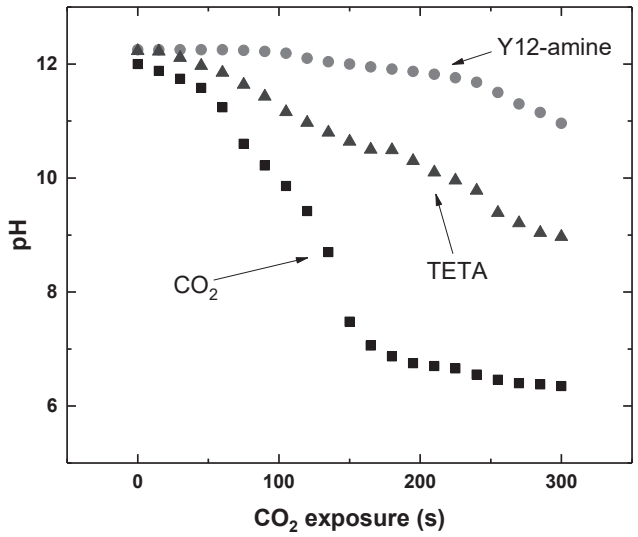

Figure 15. *pH versus time of CO_2 exposure of triethylene triamine (TETA) (triangle), Y12-amine (circle) and without amine (square) in 0.02 M NaOH. pH measurements were done with a standard deviation of ± 0.2 unit. The concentration of Y12-amine and TETA, when present, was 28.9 mM, which is above CMC (CMC = 0.27 mM) (**Paper I and II**). Reprinted from Paper II © with permission from Wiley.*

magnitude. Finally, in the presence of a self-assembling amine, Y12-amine, above the CMC, pH was steady for ~120 seconds before it started to decrease in magnitude. This pH decrease was in lower magnitude in the presence of the self-assembled Y12-amine compared to the non-self-assembled TETA. A tentative explanation for this difference in behaviour is that the surface active Y12-amine, present at the CO_2-water

interface formed Y12-carbamate and thus, delayed dissolution of CO_2 in the bulk. On the other hand, regarding TETA, which is not surface active, the carbamate formation most likely occurred in the bulk. The formation of carbamate of the self-assembled Y12-amine gave a higher yield (65 %) compared to the non-self-assembled, TETA (yield: 30 %) while maintaining pH above 11.5.

Role of the structure of the amine in the formation of carbamate

A variety of amines with different structures were exposed to CO_2 to study the transformation to the corresponding carbamate. As already discussed, the formation of anionic carbamates is only possible at pH well above the pKa of the ammonium species. The study was performed in 0.02 M NaOH and the pH was carefully monitored. The amines that were studied are shown in Figure 16.

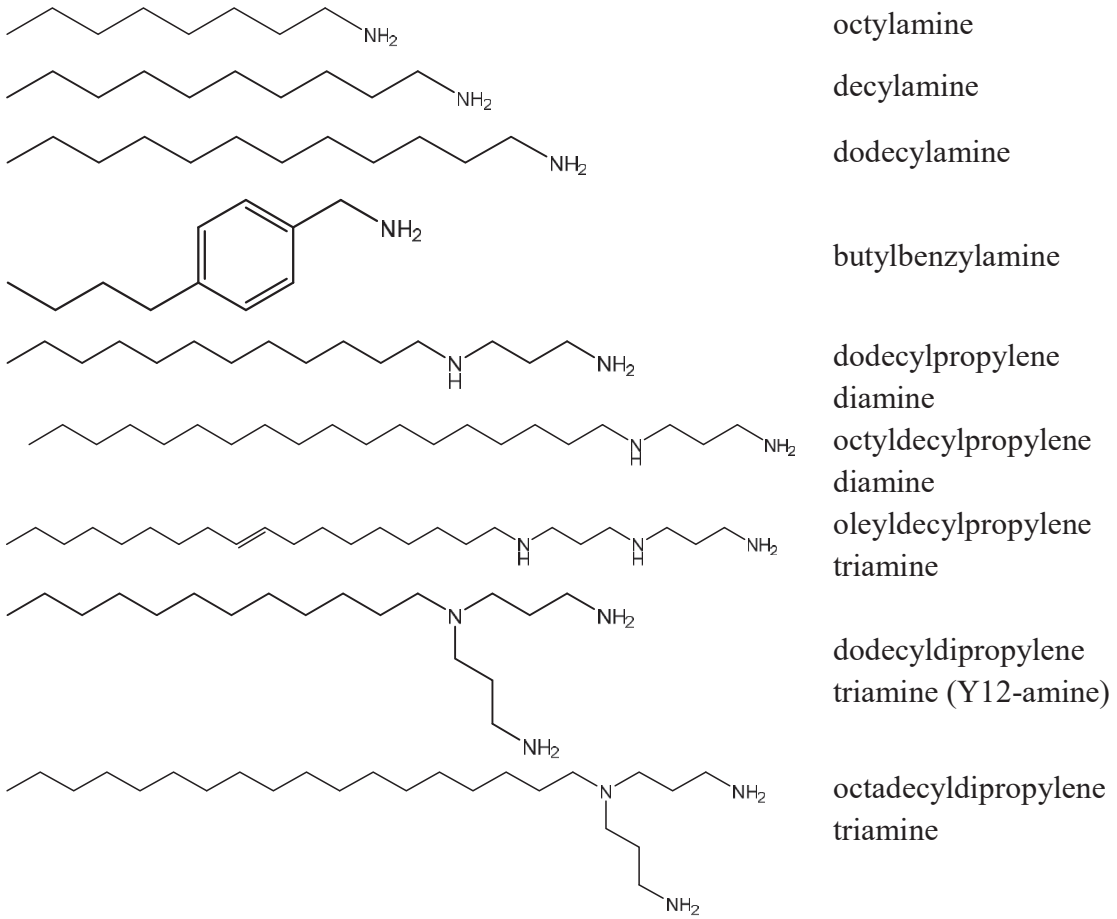

Figure 16. *Structure of the amines investigated in this research for the formation of carbamates.*

Alkyl amines solubility in water is strongly dependent on the pH. At pH above the pKa, amines are de-protonated and neutral, limiting their solubility. Only octylamine, butylbenzylamine and dodecylpropylene diamine were dispersible in the sodium hydroxide aqueous solution. The other alkyl amines had limited solubility, which reduced their ability to form carbamates. Furthermore, only the branched dodecyldipropylene triamine, the Y-shaped amine (Y12-amine), formed anionic carbamate, which did not precipitate. After 120 seconds of CO_2 exposure at the surface of the aqueous sodium hydroxide solution of Y12-amine, the conversion of Y12-amine to sodium Y12-carbamate was 65% and no sign of precipitation was observed. Octylamine converted to sodium octylcarbamate with a yield of 83% after 120 seconds of CO_2 exposure, but precipitated after 20 minutes at room temperature. Butylbenzylamine and dodecylpropylene diamine became hazy and precipitated directly after exposure to CO_2. A tentative explanation to why the Y12-amine did not precipitate after exposure to CO_2 is its favourable molecular structure. The Y-shaped structure of sodium Y12-carbamate does not favour close packing, which enhances its solubility in water. Octylcarbamate precipitated after 20 minutes, probably due to its linear structure.[8] One factor that may have contributed to the precipitation of sodium octylcarbamate is the formation of intermolecular hydrogen bonding between the carbamate moieties (see Figure 17). Bordes *et. al.* reported that the intermolecular hydrogen bonding of the amide groups in *N*-lauroylglycinate led to tighter packing at the air-water interface and hydrophobic surfaces but also increased the tendency to precipitate.[79]

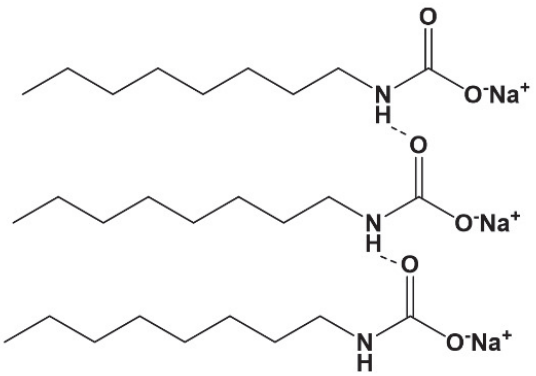

Figure 17. *Proposed mechanism for intermolecular hydrogen bonding of sodium octyl carbamate at pH 12.*

Exposure of Y12-amine to CO_2 at different pH values

The formation of the anionic Y12-carbamate is central to the design of the de-colouring method discussed in this thesis. In Figure 18, the visual appearance of the samples of Y12-amine at different pH values after CO_2 exposure is shown. Two pKa values of the Y12-amine have been determined; one at ~6.9 (the tertiary amino group) (called in this thesis pKa_1) and at ~9.0 (the two primary amino groups) (called in this thesis pKa_2).[(1)] [80] However, the three amino groups in Y12-ammonium will affect each other due to the short distance between them and the tertiary amino group has the lowest pKa because of the two electron withdrawal primary amino groups. It is only the primary amino groups of Y12-amine that can react with CO_2 and form Y12-carbamates. The sample with Y12-amine at a pH below both pKa values (pKa_1 and pKa_2) (to the left) was protonated, thus not susceptible to react with CO_2, but in the sample at a pH above the upper pKa_2 (to the right) the anionic carbamate was formed.

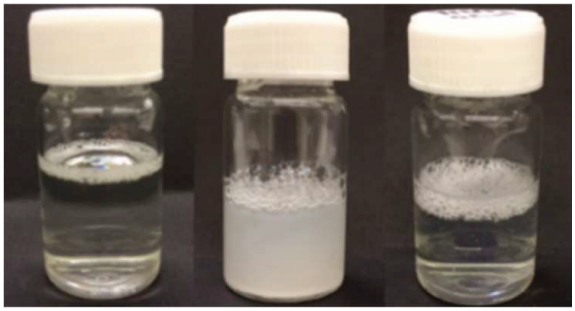

Figure 18. *Visual appearance of Y12-amine after CO_2 exposure at 28.9 mM at pH 3* ***(left)****, neutral pH* ***(middle)*** *and pH 12* ***(right)****. Reprinted from Paper I © with permission from Elsevier.*

The sample, in which pH (pH ~ 9) was not adjusted (in the middle), was cloudy and contained precipitated material. Presumably, this occurred as the ion-pair of alkyl ammonium-alkyl carbamate formed due to van der Waals interactions between the alkyl chains lead to the formation of a catanionic surfactant. The Y12-amine and the subsequent species discussed in this thesis are shown in Figure 19.

The hydrolysis of anionic Y12-carbamate was also investigated. When exposing the surface of the aqueous solution to N_2 at 95 °C, 88% of Y12-carbamate was converted to the initial amine within 3 hours (**Paper I**).

[(1)]pKa values are affected by the surrounding environment. For example, if one of the primary amino groups become protonated, the pKa's values of the other amino groups in the molecule will be affected and therefore, the pKa's values should be considered as a guideline rather than absolute values.

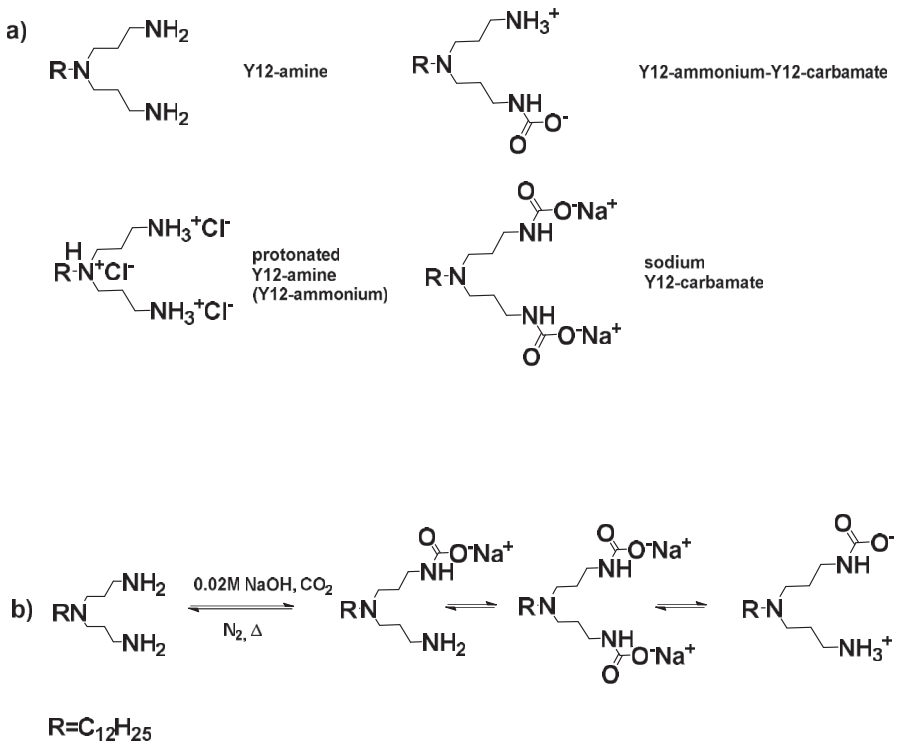

Figure 19. (a) *The different species based on Y12-amine, discussed in this thesis.* ***(b)*** *Y12-amine reacts with CO_2 to form various Y12-carbamate species depending on time of CO_2 exposure.*

Physicochemical properties of the Y12-amine and the analogous carbamates

Table 1 shows the CMC values of the Y12-amine and its carbamates at different pH values. The following unexpected trend was found:

protonated Y12-amine (pH 3) > Y12-amine (pH 12) > Y12-amine (not pH adjusted)

Based on the pH dependence of the apparent charge of the Y12-amine, one would have expected the following trend:

protonated Y12-amine (pH 3) > Y12-amine (not pH adjusted) > Y12-amine (pH 12)

Table 1. *Values of CMC, area per molecule determined from the surface tension vs. log (surfactant concentration) plot according to Gibbs adsorption equation, and surface tension at the CMC (γ) at 24 °C for the different systems studied. Reprinted from Paper I © with permission from Elsevier.*

Sample	pH	CMC (mM)	Gibbs pre-factor	Surface area per molecule ($Å^2$)	Value of surface tension at the plateau (mN/m)
Y12-ammonium [(a)]	3	1.45	3	88	33.6
Y12-amine [(b)]	not pH adjusted [(d)]	0.27	1.5	32	32.6
Y12-amine [(b)]	12	0.47	1	37	32.5
Y12-ammonium-Y12-carbamate	not pH adjusted [(e)]	0.10	N/A [(f)]	N/A [(f)]	28.9
Sodium Y12-carbamate [(c)]	12	0.97	2.3	71	40.6

[(a)] in presence of 10 mM Na_2CO_3, pH adjusted with HCl.
[(b)] without Na_2CO_3 as it would induce carbamate formation.
[(c)] Na_2CO_3 formed during CO_2 exposure, pH adjusted with NaOH
[(d)] Before CMC determination pH =7 and after pH=10.4.
[(e)] Before CMC determination pH=7 and after pH =9.1.
[(f)] N/A: Not Applicable.

A tentative explanation for this discrepancy is that the Y12-amine, at pH 12, at the air-water interface, transforms readily to sodium Y12-carbamate by reacting with atmospheric CO_2.[80, 81] During the CMC determination, a drift in surface tension of Y12-amine at pH 12 was observed before equilibrium was reached potentially suggesting formation of the Y12-carbamate. Furthermore, it has previously been reported by Burns *et al.* that amines can react with CO_2, present in the air (~ 400ppm)[82] and form carbamate species.[81] Moreover, the CMC value of 0.27 mM for the Y12-amine in Milli-Q water was in agreement with the value reported by Oskarsson *et al.* (CMC = 0.17 mM).[80] As expected, the Y12-carbamate at pH 12 had a higher CMC value (0.97 mM) than the ion pair of Y12-ammonium-Y12-carbamate (0.10 mM).

The area per molecule of the Y12-amine was determined at different pH and was found to be smallest at pH close to the pKa_2 (marked as *not pH adjusted* in Table 1).

The same trend for area per molecule was reported for fatty acids by Kanicky *et al*.[83] They suggested that this was related to a strong dipole-ion interaction between the adjoining carboxyl groups and the ionized molecules close to the pKa (~50% of the molecules are ionized at a pH close to the pKa, resulting in close packing of the molecules). In the case of the Y12-amine, the observed increase in area per molecule at pH above pKa_2 (pH 12), when one would expect a decrease can also be explained by the formation of anionic Y12-carbamate.

The area per molecule determined by the interpretation of the isotherm of adsorption with the formalism suggested by Gibbs are reliable for non-ionic surfactants. The situation is, however, less clear for ionic surfactants (see equation 6). This relates to the uncertainty of whether complete dissociation of the counterion occurs. For a monovalent ionic surfactant with complete dissociation, Gibbs pre-factor, *n*, is assumed to be 2 since the surfactant contains two ionic species: the surfactant and counterion. If the counterion is not moving freely, the surfactant and the counterion are not considered to be two independent species and thus a value less than 2 should be used. In the case of the Y12-ammonium (100% protonated Y12-amine) at pH 3, which consists of two protonated primary amines, one protonated tertiary amine, and one counterion, the molecule consists of four solute species. If one assumes full dissociation of the counterion, the Gibbs pre-factor *n* would be 4. However, the corresponding area per molecule would be too large. Therefore, it has been assumed that it is more realistic to use a value between 2 to 3 for surfactants with multiple charges, such as for gemini surfactants. No clear explanation can be given to as why this is the case, but it has been widely discussed in the literature.[69, 84 85, 86] It has been suggested that the binding of the counterion could be the major consequence. Therefore, it is suggested that neutron scattering is a better choice to determine the area per molecule since it is a direct method to measure the surface excess.[87]

For Y12-amine, not pH adjusted (pH ~ 9), a value of n=1.5 was chosen, since at pH close to pKa_2, hypothetically, approximately 50% of the primary amino groups is protonated (ionized) and the tertiary amino group (pKa_1) is deprotonated. Finally, a value of n=2.3 was assumed for sodium Y12-carbamate, related to the 65% yield of Y12-carbamate from Y12-amine (n=2 for mono-carbamate surfactant and n=3 for di-carbamate surfactant).

Influence of the gas phase on the determination of CMC of Y12-amine

Unexpectedly, a drift in surface tension during the CMC determination of the Y12-amine at pH 12 was observed. The drift was more pronounced at concentrations below the CMC. To investigate the reasons for this drift in surface tension at the air-water interface, the CMC was also determined at the N_2-water interface and by ^{1}H-NMR spectroscopy. The reason for comparing the CMC determined by pendant drop analysis with that obtained by ^{1}H-NMR spectroscopy was twofold: 1) the gas to liquid volume is larger with the pendant drop technique compared to the NMR tube; 2) tensiometry is an indirect method to determine CMC while NMR spectroscopy is a direct method since it monitors the micellisation directly in the bulk. In Table 2, the CMC values of the Y12-amine at different pH values and interfaces, determined by tensiometry and ^{1}H-NMR spectroscopy, are presented. The CMC values of the Y12-amine in MilliQ water were similar at the different gas-water interfaces as determined by the pendant drop method but were slightly higher when determined by ^{1}H-NMR spectroscopy. This could be due to the difference in the techniques used, particularly as tensiometry promotes the use of a x-log scale of concentration which is prone to larger uncertainties. In contrast, the CMC values of the Y12-amine at pH 12 differed almost by a factor of 5 depending on the interface studied (see Table 2). Furthermore, the CMC value of the Y12-amine at pH 12 (0.09 mM) determined by ^{1}H-NMR spectroscopy (N_2 rich atmosphere) agreed with the CMC value (0.09 mM) determined at the N_2-water interface by the pendant drop method.

Table 2. *CMC (in mM) of the Y12-amine determined by the pendant drop method and by ^{1}H-NMR spectroscopy. Reprinted from Paper II © with permission from Wiley.*

Sample	Pendant drop (N_2/water interface)	Pendant drop (air/water interface)	NMR (chemical shift)
Y12-amine in MilliQ water	0.27±(0.03)	0.27±(0.03)	0.35±(0.04)
Y12-amine at pH 12	0.09±(0.01)	0.47±(0.05)	0.09±(0.01)

6.1.2 Interfacial behaviour

Formation of the anionic Y12-carbamate at the CO_2-water interface

The pronounced tendency of the Y12-amine to form carbamates motivated further investigations at the CO_2-water interface by surface tension measurements. The surface tension of the Y12-amine solution was measured using the pendant drop technique, for which the atmosphere could be controlled (see Figure 8).

Initially, reference experiments were performed. All the surfactant solutions were prepared in borate buffer (0.1 M). First, the dynamic surface tension of only borate buffer was monitored during CO_2 and N_2 exposure to ensure that no variation occurred when changing gases. The variation was found to be less than 1.0 mN/m, which indicated that the surface tension of the borate buffer was not affected by exposure to the gases. This is also in agreement with findings by Wűstneck *et al.,* who reported that dissolution of different gases and vapours under atmospheric pressure at a water surface did not change the surface tension.[88]

Moreover, given the large surface to volume ratio of the droplet, in comparison with the conditions used during the preparation of Y12-carbamate in bulk, where only the surface of the beaker containing the Y12-amine aqueous solution is exposed to a stream of CO_2, the experimental set-up was thoroughly assessed. A flow rate of 40 ml/min was used, allowing rapid gas exchange in the chamber. The changes in pH over time, when the drop (~5-10 µl) was exposed to CO_2, were monitored by following the colour change of a pH-responsive dye, indigo carmine, in borate buffer (see Figures 20 (a) and 20 (b)).

Despite the presence of the buffer, the pH decreased from 12.4 to 11.5 within ~25 seconds of exposure to CO_2 at 40 ml/min (see Figure 20 (c)). The dye was not surface active, and the surface tension remained unaffected when the interface was exposed to CO_2 and N_2. Attempts to measure the surface tension of the dye in the presence of the Y12-amine failed due to precipitation of amine. The decrease in pH over time in the presence of the Y12-amine could not be monitored. However, the presence of a monolayer of surfactants at the gas-water interface has been shown in several studies to reduce the diffusion rate of gas molecules across the interface.[89, 90] Consequently, it can be assumed that the pH did not decrease during the time frame of the following experiments.

The dynamic surface tension of non-CO_2 responsive surfactants such as alcohol ethoxylate (C10-8EO) and sodium dodecylsulfate (SDS), were also evaluated during CO_2 and N_2 exposure. No significant changes of the surface tension could be observed (**Paper I**).

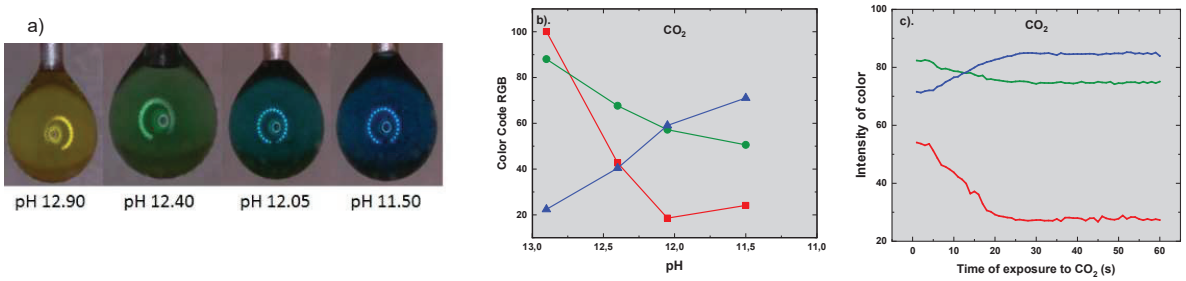

Figure 20. *The change in pH as a function of time of CO_2 exposure to the bulk phase was monitored by following the change of colour of the pH indicator indigo carmine.* ***(a)*** *Picture of the pendant drop shifting color with pH. The dye is yellow at pH 13 and blue at pH 11.* ***(b)*** *The color code RGB versus pH (square=red, circle=green and triangle=blue)* ***(c)*** *Normalised RGB channels values versus time during CO_2 exposure of the pendant drop in the chamber. Reprinted from Paper I © with permission from Elsevier.*

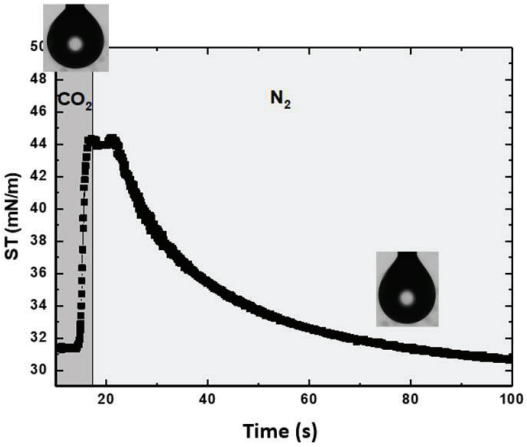

Figure 21. The *Y12-amine (concentration of 0.27 mM) in 0.1 M borate buffer at pH 12. Switching of gases is marked in the figure. Note that the fluctuation around 20 seconds is due to local variations of the atmosphere surrounding the droplet that is unavoidable with the current experimental setup (The standard deviation of the measurements was ± 1 mN/m). Reprinted from Paper I © with permission from Elsevier.*

In Figure 21, the surface tension of the Y12-amine (concentration of 0.27 mM, at CMC) as a function of CO_2 exposure in a borate buffer solution (0.1 M) is presented. At pH 12, the introduction of CO_2 into the chamber induced a rapid increase of the surface tension of the Y12-amine, from ~31.3 mN/m to ~44.0 mN/m, followed by a short plateau. At the plateau the gas was changed to N_2 and the surface tension decreased to ~31.0 mN/m. The variation in surface tension is similar in magnitude to what has previously been reported for pH-responsive surfactants where CO_2 has been used as pH trigger.[91, 92]

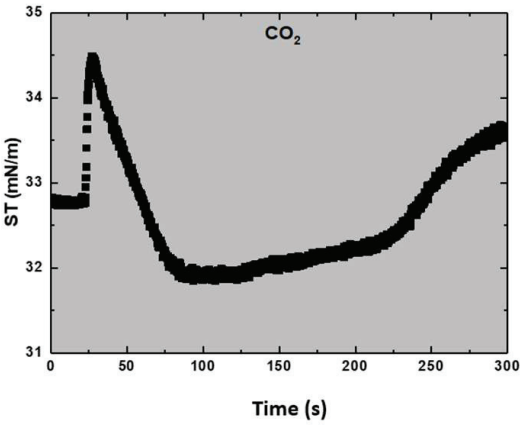

Figure 22. *Dynamic surface tension of Y12-amine (28.9 mM) in 0.1M borate buffer at pH 12 versus time of CO_2 exposure (40 ml/min). Standard deviation of the measurements was 0.3 mNm^{-1}. Reprinted from paper II © with permission from Wiley.*

Another interesting aspect was to study the change in dynamic surface tension of Y12-amine over a longer time of CO_2 exposure. In this case, the pH decreased below pH 11.5. In Figure 22, the dynamic surface tension of the Y12-amine (28.9 mM) in 0.1 M borate buffer at pH 12 versus time of CO_2 exposure is shown. First, an increase in dynamic surface tension followed by a decrease can be observed, in a similar manner to that shown in Figure 21. However, surface tension decreased below the starting value, indicating formation of a species more surface active than prior to the CO_2 exposure. One possibility is that the ion-pair of Y12-ammonium-Y12-carbamate was formed. After exposure of CO_2 (> 250 s), the surface tension increased again, which is presumably related to precipitation of the ion-pair.[8] It is important to note that the salt concentration was high, which also promoted precipitation.

Finally, the Y12-amine (28.9 mM) was exposed to CO_2 at various pH values. At pH 3, the dynamic surface tension remained unaffected when the interface was exposed to CO_2. This was expected as the Y12-amine was most likely fully protonated at pH 3 and thus not susceptible to react with CO_2. At pH 9, the dynamic surface tension first increased slightly (~1.0 mN/m) and then decreased below the starting value. In this case, the pH was close to the pKa_2 of the primary amino groups of the Y12-amine (pKa_2= 9.0)[80] and predominately the ion-pair Y12-ammonium-Y12-carbamate was formed (**Paper I**).

As indicated earlier, (see section *"Physicochemical properties of the Y12-amine and the analogous carbamates"*), the Y12-carbamate was less surface active than the Y12-amine at pH 12. An increase in the dynamic surface tension during CO_2 exposure of Y12-amine at pH 12 is in line with this observation and suggests that the rate of formation of anionic Y12-carbamate was higher than the adsorption rate of Y12-amine at the CO_2-water interface.

Figure 23 shows an illustration of the exchange of anionic sodium Y12-carbamate and Y12-amine at the gas-water interface at pH 12 during CO_2 and N_2 exposure. At the surface of the newly formed drop of an alkaline solution of the Y12-amine, the Y12-amine is adsorbed. After CO_2 exposure, the anionic Y12-carbamate is formed which is less surface active than the Y12-amine. Therefore, the anionic Y12-carbamate desorbs from the surface and change places with the more surface active Y12-amine. The actual amount of surfactant is much higher in bulk than at the interface.

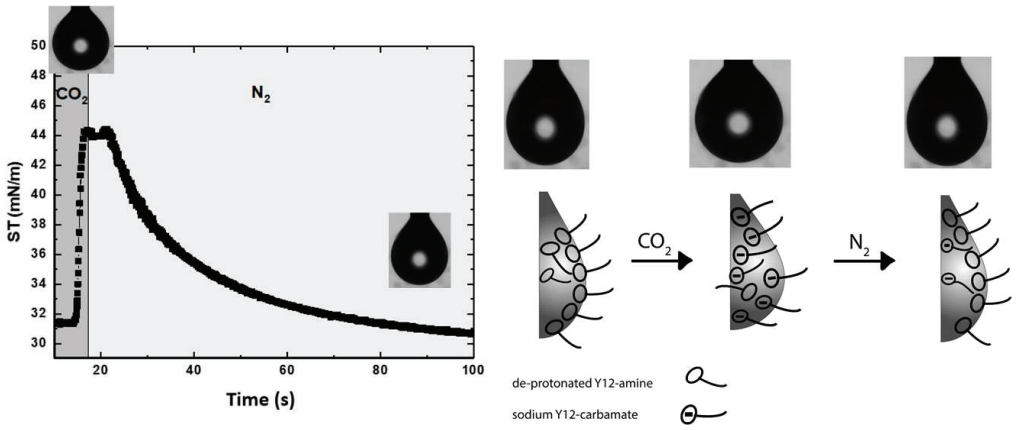

Figure 23. *Illustrative image of the exchange of the anionic sodium Y12-carbamate and the Y12-amine at the gas-water interface at pH 12 during CO_2 and N_2 exposure.*

6.2 Switchable carbamate surfactant applied to colloidal dispersions (Paper III)

In this section, the preparation of the pigment dispersion and the efficiency of the switchable carbamate surfactant to stabilise and reversibly flocculate hydrophobic particles is discussed (**Paper III**). In order to achieve the reversible colouring of a textile fabric, it was essential to understand the re-dispersion and flocculation behaviour of the pigment dispersion. Two different particles were evaluated: a micron-sized particle consisting of hydrophobically modified silica (5 μm, C18 grafted), and a nano-sized organic pigment (primary particle size 60 nm, pigment PV23). These two types of particles were selected for their hydrophobic character, which make them difficult to disperse in water.[40] Additionally, pigment Yellow 74, which is dispersible in water, was also used.

6.2.1 Formation of Y12-carbamate when adsorbed on nanoparticles

A central aim of this thesis was to evaluate whether the Y12-carbamate could be formed *in-situ* via conversion of the Y12-amine when adsorbed at the surface of the solid nanoparticles. This was investigated by studying the streaming potential as a function of CO_2 exposure in a 0.01 M NaOH solution (pH 12) of a 0.1 w/w% dispersion of pigment Yellow 74 with Y12-amine as a dispersing agent.

As a reference, the pigmented nanoparticles stabilized by a non-CO_2 responsive non-ionic surfactant (C8-E10) were also studied. In Figure 24, the streaming potential of Yellow 74 with different surfactants versus the time of CO_2 exposure is shown. The negative streaming potential significantly increased during the CO_2 exposure of the pigment with Y12-amine (4 mM). This is in contrasts to the streaming potential with the non-ionic surfactant, which was unaffected during CO_2 exposure. The increase in negative streaming potential indicated that the anionic Y12-carbamate was formed from the Y12-amine and induced negative electrostatic stabilisation. This was expected since the Y12-amine was previously shown to be CO_2 responsive while the non-ionic surfactant was non-responsive (see section *"Interfacial behaviour"*). It is important to note that the PCD values are not absolute but only relative. The PCD values are very high, probably due to the movement of the particles induced by the oscillating piston in the measuring cell.

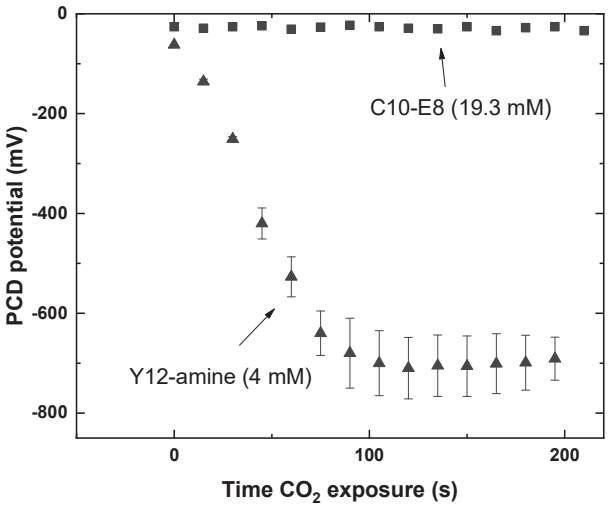

Figure 24. *Streaming potential measurements versus time of CO_2 exposure of 0.1 w/w% pigment Yellow 74 with alcohol ethoxylate (C10-E8) and different concentrations of Y12-amine at pH 12. The values presented in the graph are mean values of three independent measurements. It is noteworthy that PCD potential values are not absolute only relative. Reprinted from Paper III © with permission from Elsevier.*

6.2.2 Effect of the concentration of the Y12-carbamate on stability

The concentration of the surfactant in the dispersed system is known to affect the stability. The optimal concentration of Y12-carbamate to stabilise 0.1 w/w% nanoparticles of pigment PV23 was determined by adding different amounts of the Y12-carbamate to the 0.1 w/w% nanoparticles. In Figure 25, the mean particle size and the electrophoretic mobility of a 0.1 w/w% nanoparticle dispersion with different concentrations of the Y12-carbamate at pH 12 are presented. The optimal concentration of Y12-carbamate to stabilise a 0.1 w/w% dispersion of pigment PV23 was ~ 4mM, as indicated by an increased negative electrophoretic mobility and a decreased mean particle size.

In these experiments the Y12-carbamate had to be prepared *ex-situ* and added to the 0.1 w/w% nanoparticle dispersion to efficiently stabilise the dispersion. Attempts to form Y12-carbamate *in situ*, in the presence of Y12-amine resulted in a less stable nanoparticle dispersion with a larger particle size. A tentative explanation for this is that the formation of Y12-carbamate is favoured at the gas-water interface compared to the solid-water interface. When the Y12-amine was adsorbed at the pigment and

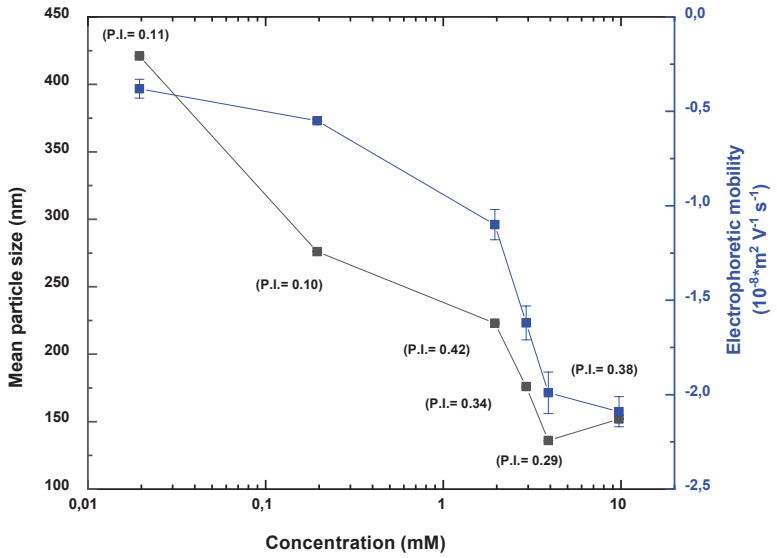

Figure 25. *Mean particle size and electrophoretic mobility versus log concentration of sodium Y12-carbamates. Reprinted from Paper III © with permission from Elsevier.*

present in solution, the conversion of the Y12-amine to the Y12-carbamate was only 30% compared to 65% when adsorbed at the gas-water interface. A possible explanation is that CO_2 (g) dissolves in the aqueous sodium hydroxide solution and decreases pH in parallel with the formation of carbamate, which protonates the amine and prevents the further formation of Y12-carbamate. At the gas-water interface, this competition is less.

6.2.3 Effect of pH on the stability of the nanoparticle dispersion

The formation and stability of Y12-carbamate have been shown to be sensitive to pH. Therefore, the stability of the nanoparticle dispersion with the Y12-carbamate (4 mM) was studied at various pH values across the range 7.2 - 10.7 (Figure 26 (a)). The particle size and electrophoretic mobility of the different samples are presented in Table 3. The stability of the nanoparticles was strongly dependent on the pH. As expected, the sample at pH 9.1, which is very close to the pKa_2 of the primary amino groups (pKa_2= 9.0), flocculated quickly due to the formation of the ion-pair Y12-ammonium-Y12-carbamate.

Surprisingly, at pH 7.2 the pigment dispersion had a low positive electrophoretic mobility. There are several possible explanations for this. At pH 7.2, Y12-carbamate

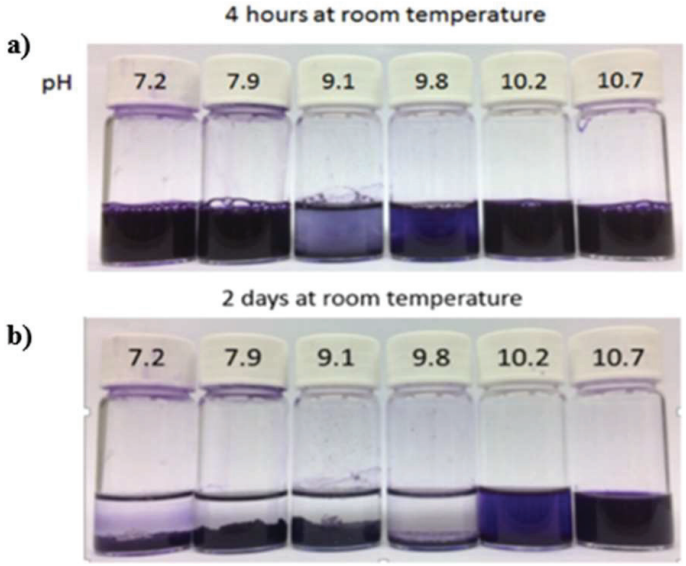

Figure 26. *Stability of nanoparticle dispersion stabilized by Y12-carbamate at different pH* ***a)*** *after 4 hours* ***b)*** *after two days. Reprinted from Paper III © with permission from Elsevier.*

(65% yield) may become protonated and, thus, uncharged while the Y12-amine (35% yield) transforms into the Y12-ammonium (cationic surfactant). In addition to forming Y12-ammonium-Y12-carbamate at pH 7.2, the Y12-carbamate undergoes hydrolysis and transforms into the Y12-ammonium. At pH 10.7, the anionic Y12-carbamate remained intact and enabled proper stabilisation. After two days at room temperature, all samples had flocculated or started to flocculate except the sample at pH 10.7 (Figure 26 (b)).

Table 3. *Mean particle size and electrophoretic mobility of a nanoparticle dispersion at different pH values, 4 hours after preparation. Reprinted from Paper III © with permission from Elsevier.*

Time (h)	pH	Mean particle size (nm)	Poly dispersity index (P.I.)	Electrophoretic mobility (10^{-8} m^2 V^{-1} s^{-1})
4	7.2	140	0.37	1.7 (±0.3)
4	10.7	134	0.33	−2.7 (±0.2)

6.2.4 Reversible flocculation of the nanoparticles

The efficiency of the carbamate surfactant to reversibly flocculate the pigment dispersion was investigated. In previous chapters, the switchable Y12-carbamate surfactant in aqueous sodium hydroxide solution was shown to revert to the corresponding amine by exposure to N_2 and heating (**Paper I**). This feature of the carbamate surfactant was employed to cycle the nanoparticles between a stable ("on") and flocculated ("off") state. In Figure 27, the mean size of the nanoparticles with the Y12-amine at pH 12 during two cycles of re-dispersion ("on") and flocculation ("off) is presented. The destabilisation process ("off") was caused by exposure with N_2 and increasing the temperature to 80 °C for 2 hours. Nanoparticles were re-dispersed ("on") again by sonication and exposure to CO_2 for 60 seconds. The mean particle size was 134 nm when the Y12-carbamate was formed *ex-situ* prior to addition to the nanoparticle dispersion. After each re-dispersion cycle, the mean particle size increased slightly, implying that the re-dispersion process becomes less efficient with an increasing number of cycles. After two re-dispersion and flocculation cycles, no further re-dispersion of the nanoparticles to a mean particle size below 400 nm was possible due to irreversible aggregation. The pH remained constant at 12 throughout the cycles. An illustration of the flocculation ("off") and re-dispersion ("on") processes is displayed in Figure 28.

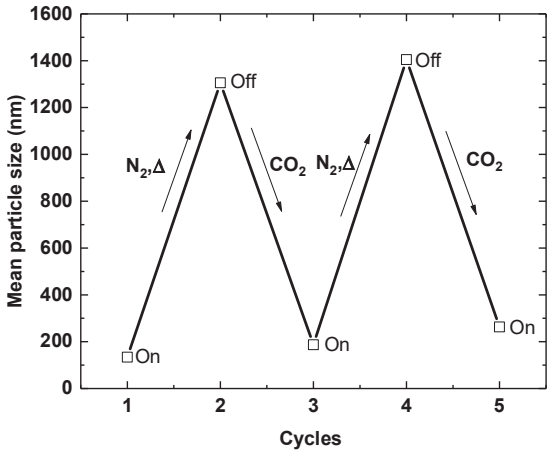

Figure 27. *Cycles of N_2 exposure during thermal heating (inducing flocculation) and CO_2 exposure (for re-dispersion of the nanoparticle dispersion). Reprinted from Paper III © with permission from Elsevier.*

In this study, the nanoparticle dispersion became unstable and flocculated at 80 °C probably due to hydrolysis of the Y12-carbamate adsorbed at the surface of the nanoparticles, which cancelled the electrostatic stabilisation. Note that the Y12-carbamate hydrolysed (88% yield) in bulk during exposure to N_2 at 95 °C. This probably means that less than 88% of the Y12-carbamate adsorbed at the particle surface was hydrolysed to achieve flocculation. This could also be the reason why the dispersion could be re-dispersed *in-situ,* thus the presence of small amount of the

Y12-carbamate could prevented irreversible aggregation. It is noteworthy that the Y12-carbamate had to be formed *ex-situ* prior to addition to the nanoparticle dispersion to introduce the first electrostatic stabilisation, whereas, during the re-dispersion process, CO_2 could be purged *in-situ* to form Y12-carbamate.

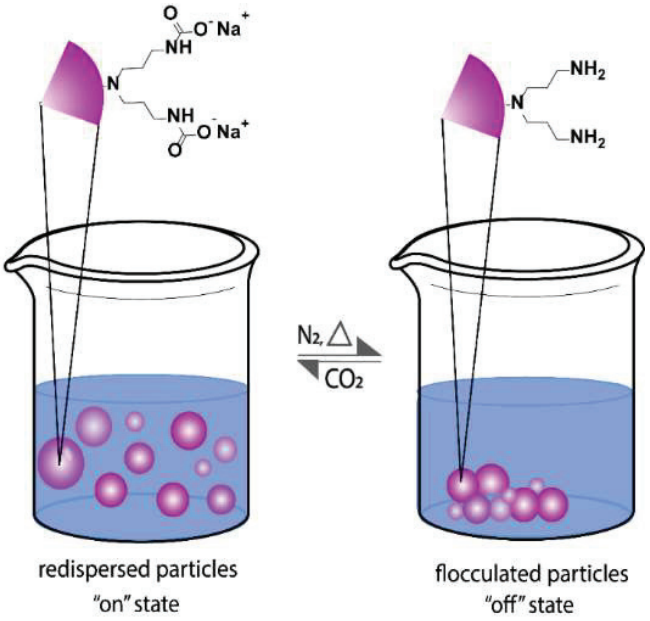

Figure 28. *Illustration of the reversible flocculation of a nanoparticle dispersion facilitated by Y12-amine. N_2 exposure during thermal heating caused flocculation and CO_2 exposure induced re-dispersion due to formation of the Y12-carbamate.*

6.3 Reversible cotton colouring (Paper IV)

In Figure 29, images of coloured (left), de-coloured (middle), and re-coloured (right) cotton fabrics are presented. The cationised cotton fabric to the left is coloured with PV23 stabilised by the Y12-carbamate, the fabric in middle is a piece of the de-coloured PV23 fabric and the one to the right is a piece of the de-coloured fabric that has been re-coloured with Heliogen Blue pigment (15:3).

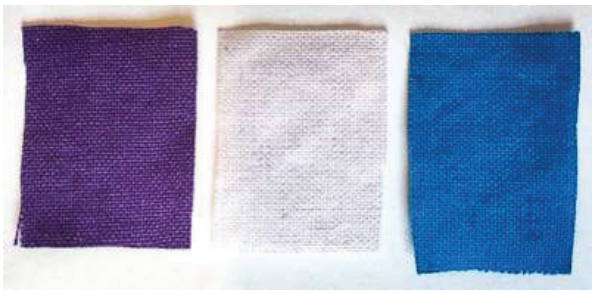

Figure 29. *Reversible adsorption of nanoparticles of pigment on cationised cotton fabric, coloured with pigment PV23* ***(left)****, de-coloured from pigment PV23* ***(middle)****, recoloured with pigment HB 15:3* ***(right)****.*

Reversible colouring of the cationised cotton triggered by carbamate surfactant

The reversible adsorption of pigment on cationised cotton was designed to occur via charge reversal of the pigment: adsorption occurred due to electrostatic attractions (and van der Waals attractions between the cotton fabric and the pigment), while desorption occurred due to electrostatic repulsion. It is well known that ionic interactions are strong and difficult to break.[8] Therefore, hypothetically, the anionic Y12-carbamate surfactant, which is both cleavable and transformable from anionic to cationic surfactant could break the electrostatic interactions between the pigment and cotton. By using Y12-carbamate as a trigger for the reversible adsorption of pigment on cationised cotton, the ionic interactions could be switched from attraction to repulsion due to the cleavable function.

Figure 30 shows an illustration of the colouring and de-colouring method strategies, which is briefly presented below.

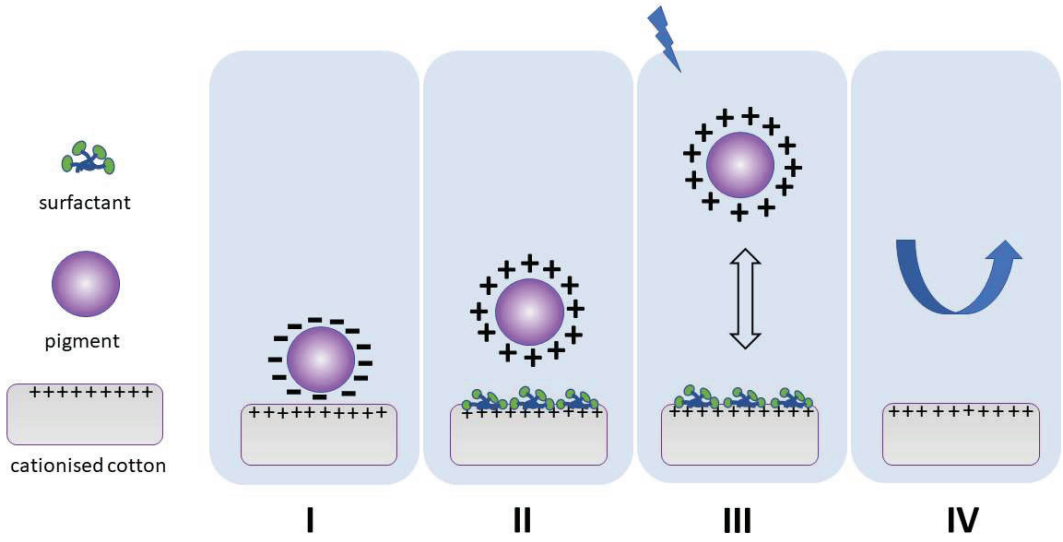

***Figure 30**. Illustration of the colouring and de-colouring mechanism. The lightning symbol represent the sonication step.*

(I) Y12-carbamate stabilises the hydrophobic pigment nanoparticles. The nanoparticles adsorb onto the cationised cotton due to electrostatic and van der Waals attraction forces.

(II) Desorption is triggered by a charge reversal of the pigment due to the acid hydrolysis of the Y12-carbamate surfactant, which induces the protonation of the Y12-amine and transforming the anionic carbamate surfactant into a cationic surfactant. In addition, a non-ionic surfactant (C11-5EO) (cloud point ~28 °C) is added to the de-colouring solution to decrease the work of adhesion by decreasing the surface free energy between the liquid and the solid (particle-water and cationic cotton-water interfaces) and to introduce the steric stabilisation of the pigment. The following requirement has to be fulfilled for the detachment of pigment from the cationised cotton surface:

$$(\gamma_{(LP)} + \gamma_{(LC)}) < \gamma_{(PC)}$$

where γ is the surface energy between liquid (L), particle (P), and cationised cotton (C). The sum of the surface free energies of the particle-water and the cationised cotton-water interfaces has to be lower than the surface free energy of the particle-cationised cotton interface.

(III) External energy in the form of ultrasonication causes the pigment detach.[67]
(IV) The fabric is rinsed with water to avoid redeposition of the pigment.[66]

6.3.1 Cationisation of cotton fabric

The cotton fabric was cationised with glycidyltrimetyl ammonium chloride, which covalently binds to the cellulose (see Figure 31).[61, 93-97] The cationic charge of the fabric was determined as ~ +0.33 (±0.04) meq/g by PCD. Additionally, to visually verify that cationisation occurred, non-cationised and cationised cotton were immersed in aqueous solution of an anionic dye (methyl orange) at pH 10. Since methyl orange also is a pH indicator, the pH was well above pKa (pKa=3.4 for methyl orange).[98] As expected, the non-treated cotton did not develop the strong yellow colour that was obtained with the cationised cotton (see Figure 32).

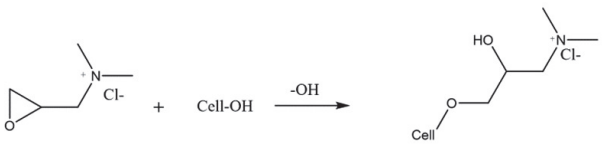

Figure 31. *Reaction of glycidyltrimethyl ammonium chloride with cellulose. Cell-OH represents the hydroxyl group of the cellulose.*

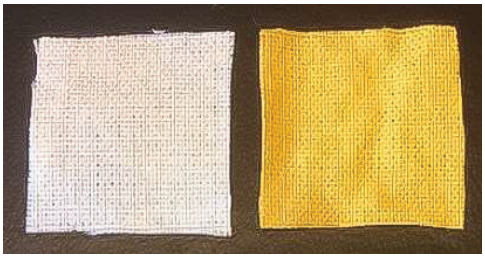

Figure 32. *Non-treated **(left)** and cationised **(right)** cotton fabric dyed with anionic orange dye at pH 10.*

Colouring of cationised cotton fabric

In Figure 33, the colouring of the non-cationised (left picture) and cationised cotton (right picture) with the Y12-carbamate stabilized pigment dispersion is presented. The colour of the cationised cotton was stronger compared to that of the non-cationised fabric, which is in agreement with other studies.[61, 97] The fabric was not coloured throughout its thickness and the center of the cross cut remained free of pigment. The pigment remains at the outermost surface for all fabrics coloured with pigment PV23 stabilised with different surfactants (see Figure 34).

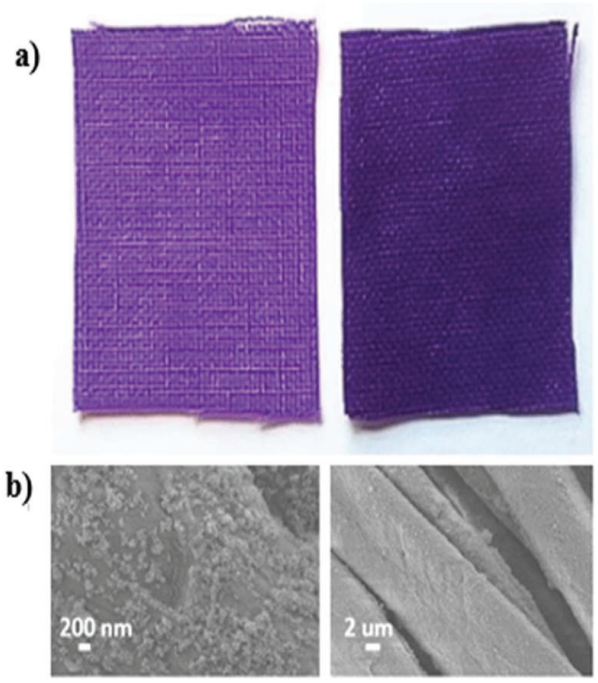

Figure 33. (a) *Image of non-treated* ***(left)*** *and cationised cotton* ***(right)*** *coloured with anionic Y12-carbamate stabilized pigment PV23* ***(b)*** *SEM image of adsorbed pigment on cationised cotton fabric.*

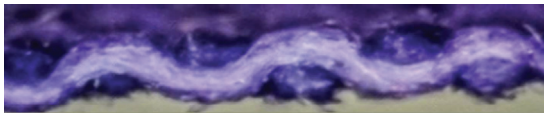

Figure 34. *Image of cross-section of the pigmented cationised cotton fabric.*

6.3.2 De-colouring of coloured cationised cotton fabric

Desorption of the pigment from the cationised cotton was induced by the hydrolysis of the adsorbed carbamate groups of Y12-carbamate. The cotton fabric was immersed in an aqueous pH 3 bath, (adjusted with hypo-phosphoric acid), at 60 ^{o}C. After the fabric had been immersed in the acidic solution for 10 minutes, the pigment had clearly started to desorb (Figure 35 (a)). However, at pH 10 at room temperature, no desorption of pigment from the cotton fabric could be observed (Figure 35 (b)). To further desorb the pigment at pH 3, the fabric was exposed to an ultrasonic disperser at an operating amplitude of 60%. The tip of the disperser was adjusted to 0.5 cm above the fabric for 10 seconds and then moved to a new location (see Figure 36). The Y12-carbamate hydrolysed in the acidic solution during heating and the resulting amine became protonated to form a cationic surfactant. Desorption occurred due to

the electrostatic repulsion between the cationised cotton and the pigment. The electrophoretic mobility of the desorbed pigment was $+3.7\times10^{-8}$ m^2 V^{-1} s^{-1} (± 0.07) compared to -2.7×10^{-8} m^2 V^{-1} s^{-1} (± 0.20) during adsorption. As can be observed in Figure 37 (a), almost all the pigment was removed from the cotton fabric.

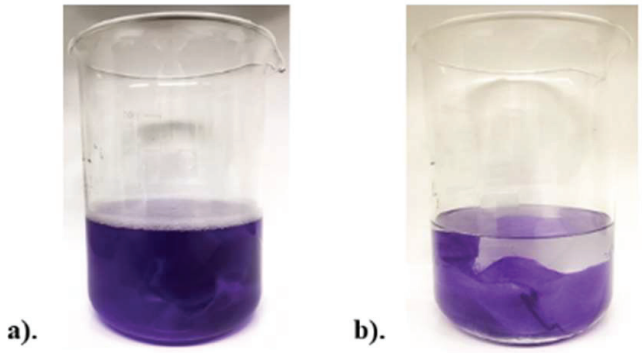

Figure 35. *De-colouring bath of coloured cationised fabric with Y12-carbamate stabilized PV23 pigment formulation* ***(a)*** *At pH 3 and 60 °C after 10 minutes.* ***(b)*** *At pH 10 and room temperature after 10 minutes.*

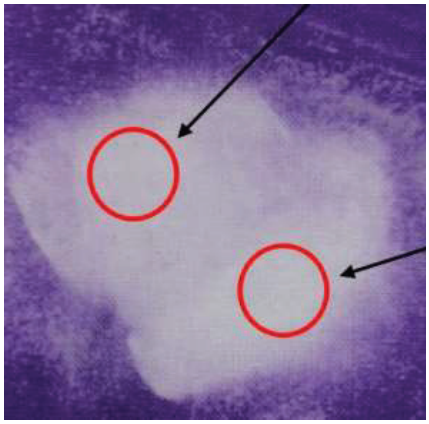

Figure 36. *Image of the de-coloured cationised cotton fabric showing the spots from the positioning of the tip of the ultrasonic disperser.*

In Figure 37 (c), the L*-values (lightness) of the non-treated, cationised, and de-coloured cationised cotton fabrics are shown. The L* value is a numerical value for the lightness (white-black) where 100 is white and 0 is black. In comparison to the original non-treated cotton, the de-coloured cotton was shown to have lost ~10% of the lightness.

In addition, the cationised cotton was also coloured with pigment PV23 dispersed with a non-switchable surfactant as sodium dodecyl sulphate (SDS). In Figure 38 (a), the coloured fabrics are shown alongside the L*, a* and b* values in Table 4 (a* and b* correspond to green-red and blue-yellow, respectively). As can be observed, the fabric with the sodium Y12-carbamate had lower colour intensity than with SDS. It was also processed for de-colouration and the result is shown in Figure 38 (b).

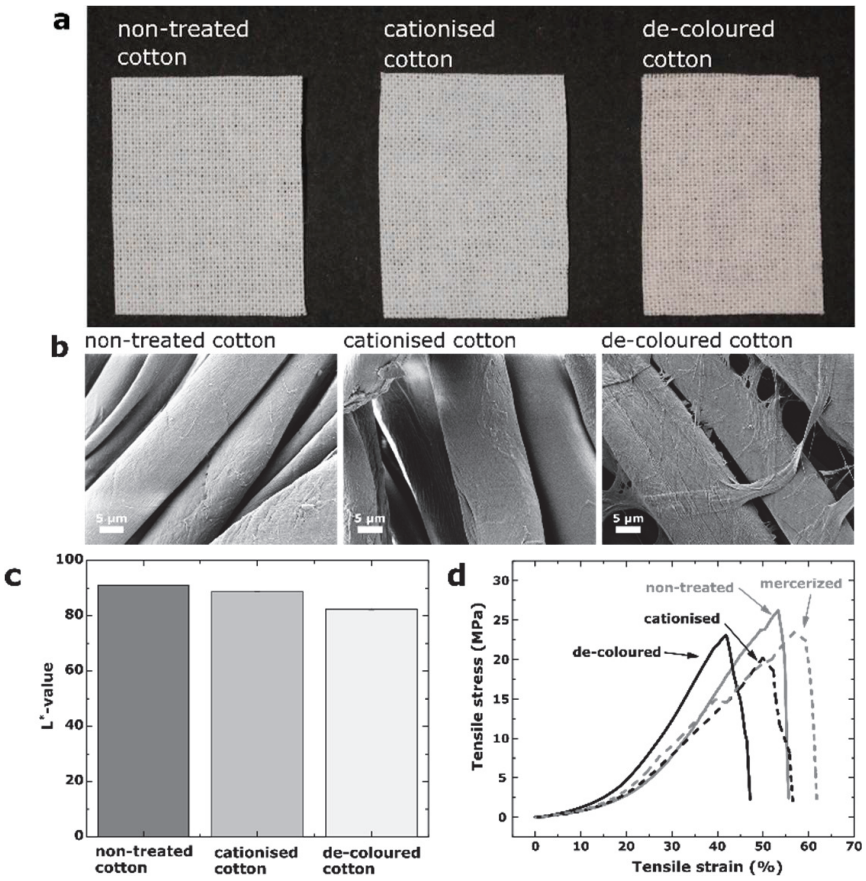

Figure 37. (a) *Non-treated cotton* ***(left)****, cationised cotton* ***(middle)*** *and de-coloured cotton* ***(right)****. **(b)** SEM image of non-treated cotton* ***(left)****, cationised cotton (middle) and de-coloured cotton* ***(right)****. **(c)** L*-values (lightness) of non-treated, cationised and de-coloured cotton. **(d)** Tensile testing curves of nontreated, mercerised, cationised and de-coloured fabrics. The cationised fabric is to be considered as the reference.*

A much larger amount of colour was removed from the fabric with Y12-carbamate than that with SDS. Unlike the Y12-carbamate, SDS does not have the dual functionality of being cleavable and switchable as the Y12-carbamate, which facilitates de-colouring. However, SDS is cleavable in strong acid. In addition, more pigment was adsorbed with SDS due to smaller pigment nanoparticle size and higher negative electrophoretic mobility, which furthermore clarifies the difficulties with de-colouring the fabric.

Table 4. *Colourimetric values of fabric coloured with pigment PV23 dispersed by the sodium Y12-carbamate and by SDS*

Sample	Sodium Y12-carbamate	SDS
L*	37.8 (±0.04)	31.2 (±0.09)
a*	30.8 (±0.04)	27.3 (±0.06)
b*	−34.0 (±0.05)	−30.4 (±0.10)

Figure 38. (a) *fabric coloured with dispersing agents sodium Y12-carbamate* ***(left)*** *and SDS* ***(right)****.* ***(b)*** *de-coloured fabric with Y12-carbamate* ***(left)*** *and SDS* ***(right)****.*

Table 5. *Particle size and electrophoretic mobility of pigment dispersions based on pigment PV23 stabilised by different surfactants.*

Sample	Size (nm)	Electrophoretic Mobility ($\times 10^{-8}$ m^2 V^{-1} s^{-1})
Y12-ammonium (pH 3) (desorbed)	181 (±0.4)	+3.7 (±0.1)
Sodium Y12-carbamate (pH 12)	131 (±0.3)	-2.7 (±0.2)
Sodium dodecyl sulfate (SDS) (pH 12)	116 (±0.1)	-3.3 (±0.1)

Tensile strength of de-coloured fabric

A highly interesting aspect of this research is the effect of the de-colourization step on the mechanical properties, and tensile strength measurements were performed. Also, non-treated cotton and mercerised cotton were studied for comparison.

The maximum tensile stress decreased from 26 (±2.0) MPa to 20 (±1.1) MPa and the tensile strain at maximum stress decreased from 53 (±1.2)% to 50 (±2.0)% during cationisation, compared to the non-treated cotton. The decreased maximum loading of the cationised fabric was in agreement with the literature.[99] Prior to cationisation, the cotton fabric was treated in 2M NaOH for 10 minutes and this treatment decreased

the tensile stress from 26 (±2.0) MPa to 23 (±1.5) MPa and the tensile strain at maximum stress increased from 53 (±1.2)% to 57 (±1.3)%. The alkali treatment could be considered as slack mercerization where no tension was applied, which would cause the fabric to shrink and result in decreased stress and increased strain.[100] This step was conducted to activate the surface hydroxyl groups for cationisation.

In Figure 37 (d), the effect of the de-colouring on the strain and the stress compared to the cationised cotton is shown. Against a reference of cationised cotton, the de-colouring method increased maximum stress by ~15% and decreased strain by ~16%. The changes in stress and strain could be related to the sonication treatment. In Figure 37 (b), SEM images of the de-coloured fabric show fibrillation of the surface fibres, which resulted in inter-fibrous cross-linking. The fibrillation of the fibres can decrease strain and the inter-fibrous cross-linking may increase the stress.

Attempts to determine an average molecular weight of the different cotton fabrics by intrinsic viscosity were also conducted. However, due to the cationisation of the cotton, the cellulose could not be dissolved by using copper diethylene triamine, which is required to perform the experiments properly.

Washing tests

To examine the colour fastness of the colouring method, washing tests at 40 °C according to ISO standard 105-C08:2010 were performed. The total colour difference (ΔE) between the coloured cotton before and after each washing cycle was measured. ΔE indirectly indicates the colour loss between each washing cycle. A ΔE value of less than 2.3 means that the human eye cannot distinguish the colour difference between two samples. In Figure 39 (left), the cumulative colour loss, indicated by ΔE across six washing cycles at 40 °C (adsorbed Y12-carbamate stabilised pigment) is shown. The colour loss between the coloured cotton (reference) and washed samples increased with each washing cycle and no clear plateau was observed. However, between each washing cycle, the colour loss was just below what is noticeable visually (ΔE< 2.3). Cationised fabric coloured with SDS stabilised PV23 pigment was also washed repeatedly and showed similar result (Figure 39 (right)). These washing tests illustrate that the loss of colour during washing is not related to a specific surfactant but rather to the fact that no binder was used to increase the pigment fastness.

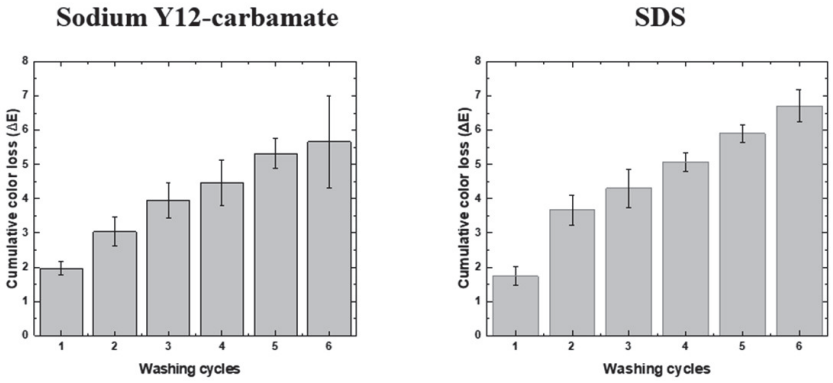

Figure 39. *Cumulative color loss (ΔE) versus washing cycles of coloured cationized fabric with pigment PV23; stabilised with the sodium Y12-carbamate* ***(left)****, stabilised with SDS* ***(right)****. Value below 2.3 are barely noticeable by the human eyes.*[75]

6.3.3 Re-colouring of cationised cotton fabric

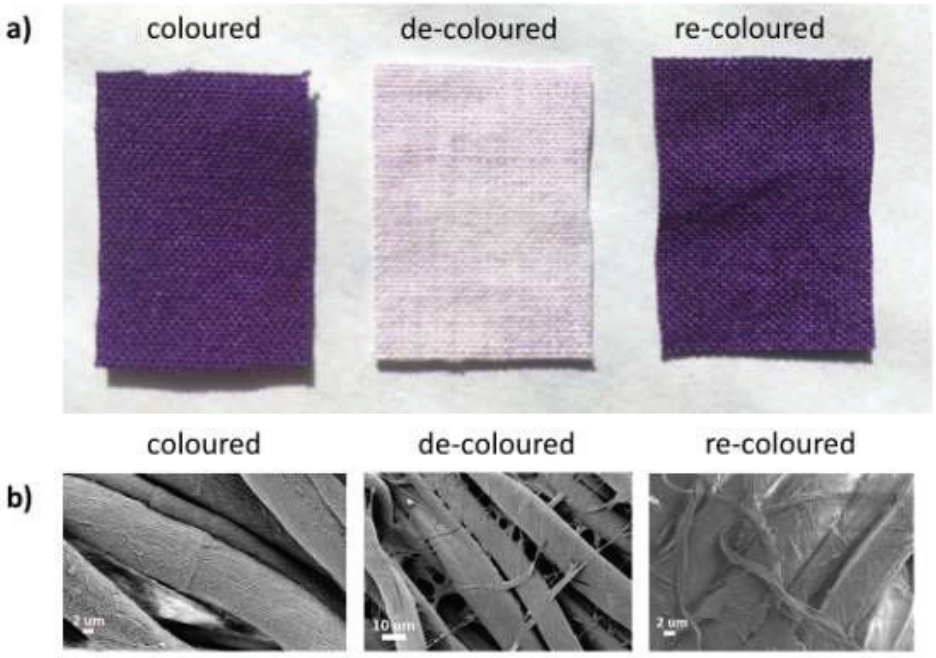

Figure 40. (a) *images* ***(left)*** *first colourisation* ***(middle)*** *de-colouring and* ***(right)*** *de-coloured, re-coloured.* ***(b)*** *SEM images first colourisation* ***(left)*** *de-colouring* ***(middle)*** *and de-coloured, re-coloured* ***(right)****.*

The cationic charge remaining on the cationised cotton after de-colourisation was 0.26 (±0.04) meq g^{-1} fibre, which was lower than the charge of the original cationised

cotton 0.33 (±0.04) meq g^{-1} fibre. However, since the de-coloured fabric possessed a high lightness (L*-value), re-colouring was possible. The de-coloured fabric was re-coloured using the same pigment dispersion, based on PV23 with adsorbed Y12-carbamate. The de-coloured cotton and a piece of the original cationised cotton were coloured in the same colouring bath. The coloured original cationised cotton was the reference, and the colourimetric values were measured and compared to those for the re-coloured fabric. Due to the loss in cationic charges, the re-coloured fabric had a lower colour strength but surprisingly, the colour loss (ΔE = 4.3 (±0.26)) was only slightly above the difference noticeable for the human eye ($\Delta E < 2.3$) (see Figure 40 (a)). As already discussed, the sonication treatment defibrillated the surface fibres during the de-colouring process, which can be observed when comparing the SEM images of the de-coloured and re-coloured cotton fabric (see Figure 40 (b)).

The de-coloured fabric was then re-coloured with another pigment based on Heliogen Blue (HB15:3) (see Figure 41). As expected, the colour strength was slightly lower for the re-coloured fabric compared to the original coloured fabric (see Paper IV, Supporting information Table S7). Finally, the de-coloured cotton was re-cationised and re-coloured with HB 15:3, and as expected, the colour strength increased (ΔE = 11.1 (±0.86)) due to the higher degree of cationisation.

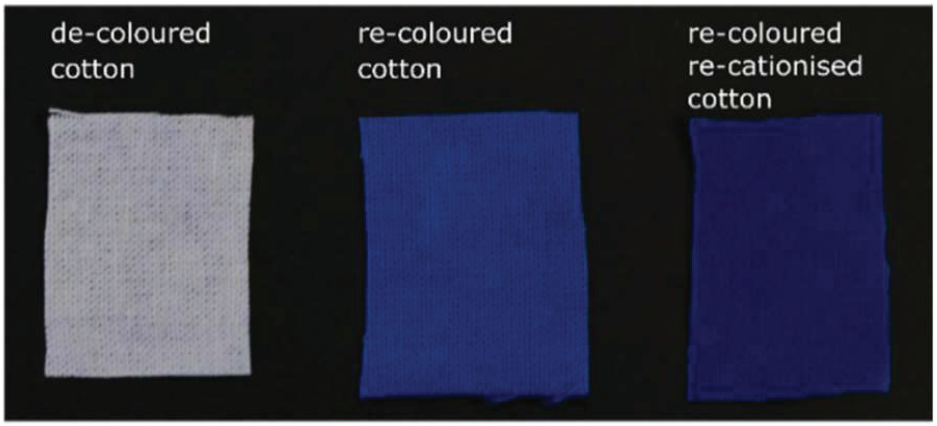

Figure 41. *Images of de-coloured cationised cotton* ***(left)****, de-coloured fabric, recoloured with HB 15:3* ***(middle)*** *and de-coloured fabric, re-cationised and recoloured with HB 15:3* ***(right)****.*

7 Conclusion

One major limiting factor in the recycling of textiles is the removal of the colour. In this thesis a de-colouring method based on the reversible adsorption of pigment on cationised cotton has been investigated and discussed. The desorption of the pigment was triggered by a switchable surfactant, sodium Y12-carbamate, adsorbed on the pigment, which under acid and heat treatment, hydrolysed and converted to cationic Y12-ammonium surfactant. Adsorption was driven by electrostatic attraction and van der Waal attractions while desorption was mainly driven by electrostatic repulsion.

The stimuli-responsive surfactant, sodium Y12-carbamate, was chosen due to its unique ability to remain stable in the pH range used in detergency, whilst hydrolysing under acidic conditions during heating. This feature was applied to control the surface charge of the pigment for colouring and de-colouring cationised cotton.

The formation of carbamates from different surface-active amines in water, along with the surface properties of carbamate surfactants, has been investigated. It was found that the structure and the solubility of the fatty amine played a central role in the formation of water-soluble carbamate surfactants. Only a Y-shaped amine, the so-called Y12-amine, could form an anionic carbamate during CO_2 exposure at pH 12. Other amines yielded anionic carbamate-based surfactants that precipitated. Furthermore, sodium Y12-carbamate could be reverted to its corresponding amine through exposure to N_2 and heat.

The surface activity of the amphiphiles were also investigated. The Y12-carbamate exhibited a lower surface activity compared to the Y12-amine, most likely due to its ionic character. At pH, close to pKa of the primary amino groups, the catanionic ion-pair Y12-ammonium-12-carbamate exhibited the lowest CMC and the highest surface activity.

Formation of the Y12-carbamate at the CO_2-water interface was also studied using the pendant drop technique. The interfacial formation of the anionic Y12-carbamate at pH 12 induced an increase in the surface tension. When CO_2 was replaced by N_2, surface tension returned to its initial value as a consequence of the replacement of the Y12-carbamate by the more surface active deprotonated Y12-amine at the interface.
The colloidal behaviour of hydrophobic pigment nanoparticles stabilised with Y12-carbamate was also evaluated. At pH > pKa of the primary amino groups of the Y12-

amine, the anionic Y12-carbamate stabilised the nanoparticles, while at pH close to pKa of the primary amino groups, the particles quickly flocculated due to formation Y12-ammonium-Y12-carbamate ion-pair. Through its hydrolysis, the Y12-carbamate enabled switching of the hydrophobic nanoparticles between a stable and a flocculated state. The anionic Y12-carbamate was formed *ex-situ* at pH 12, before the addition to the nanoparticle dispersion to electrostatically stabilise the particles. Flocculation of the particles was induced by cleavage of the carbamate groups by exposure to N_2 and heating to 80 °C, which regenerated the deprotonated Y12-amine. The nanoparticles could be re-dispersed by sonication and subsequent exposure to CO_2. The cycle was repeated twice.

Finally, reversible adsorption of the pigment stabilised by Y12-carbamate on cationised cotton was evaluated. The adsorption of the pigment mainly occurred due to electrostatic attraction and van der Waals interactions. In the de-colouring step, or desorption of the pigment, the Y12-carbamate underwent acid hydrolysis and reverted to the amine and transforming into a cationic surfactant (Y12-ammonium). This introduced electrostatic repulsion between the pigment and the cationised cotton surface. For desorption or de-colouring to occur, the repulsive forces had to be stronger than the attractive forces, and external energy had to be added in the form of ultrasonication. The electrophoretic mobility of the pigment prior to adsorption was -2.7×10^{-8} m^2 V^{-1} s^{-1} while the desorbed pigment at pH 3 had an electrophoretic mobility of $+3.7\times10^{-8}$ m^2 V^{-1} s^{-1}. The mechanical properties of the de-coloured fabric were affected, the maximum tensile stress increased by ~15% and the strain decreased by ~16% compared to cationised cotton.

8 Outlook

More studies are needed to completely understand the new colouring method with the embedded de-colouring function based on the carbamate surfactant. The most relevant aspects are summarised below

- ✓ Determine carbamate species at different pH values. The most stable form is the ion-pair Y12-ammonium-Y12-carbamate and the question is whether the ion-pair is also present at a pH above 11.5. NMR analysis indicates that the species may be present at pH 11.5 at concentrations above the CMC of the Y12-carbamate but not at a pH above 12 at concentrations above the CMC.

- ✓ Investigate the stability of sodium Y12-carbamate at different pH values.

- ✓ Study the effect of different electrolyte concentrations on the stability of the pigment dispersion and during the colouring and de-colouring process. This should be investigated at different water hardness and different detergent content.

- ✓ Verify the method with different textiles and pigments

For the purpose of the study, Y12-amine was extensively investigated. This led to a better understanding of the carbamate chemistry linked to the development of a reversible colouring process. However, for various reasons, among, which some environmental and toxic concerns, other amines should be explored, preferably bio-sourced.

Abbreviations

CMC	Critical Micelle concentration
COD	Chemical oxygen demand
CP	Cloud point
CPP	Critical packing parameter
DLS	Dynamic light scattering
EPTAC	2,3-epoxypropyl trimethylammonium chloride
HB 15:3	Phthalocyanine Blue pigment
NMR	Nuclear Magnetic Resonance
PCD	Particle Charge Detector
PV23	Dioxazine violet pigment
SEM	Scanning electron microscopy
SDS	Sodium dodecyl sulphate
TEG	Triethyleneglycol

9 Acknowledgements

FORMAS is acknowledged for financial support.

A warm acknowledgement to:

My supervisors Romain Bordes and Lars Nordstierna for all interesting scientific discussions and valuable coaching during the writing process. Your feedback is much appreciated.

My co-supervisors Hanna de la Motte and Marie Syren for all interesting scientific discussions and reviewing the thesis.

My examiner Anders Palmqvist.

Rebekah Hailes for reviewing my thesis. You will for always be my angel. I don't know what I would had done without you.

Krister Holmberg for scientific discussions and reviewing my thesis.

Frida Andersson for all administrative help.

Anders Mårtensson for performing the SEM analysis.

Krzysztof Kolman and Frida Iselau for all scientific discussions.

Leo Svenningsson for all computer related support.

Hanna Härelind for all support related to the study.

Sanna Björkegren and Archana Samanta for all valuable discussions and support.

Zareen Abbas for all scientific discussions.

Hans Oskarsson for interesting scientific discussions.

All former and present colleagues at TYK.

My family, Mikael, Emil and Fanny for being so patient and supportive during the writing process.

10 References

1. Sandin, G., and Peters G.M., *Environmental impact of textile reuse and recycling – A review.* Journal of Cleaner Production, 2018. **184**: p. 353-365.
2. Zamani, B., et al., *Hotspot identification in the clothing industry using social life cycle assessment—opportunities and challenges of input-output modelling.* International Journal of Life Cycle Assessment, 2018. **23**(3): p. 536-546.
3. Roos, S., Sandin, G., Zamani, B., Peters, G.M., *Environmental Assessment of Swedish Fashion Consumption. Five Garments - Sustainable Futures.* Mistra Future Fashion, 2015.
4. Alwood, J.M., Laursen, S.E., de Rodriquez, C.M., Bocken, N.M.P., *Well Dressed? The Present and Future Sustainability of Clothing and Textiles in the United Kingdom.* University of Cambridge, Institute of Manufacturing, Cambridge, UK, 2006.
5. EC, *Directive 2008/98/EC of the European Parliament and of the Council of 19 November 2008 on waste and repealing certain Directives (Text with EEA relevance).* 2008.
6. Brown, P., Butts, C.P. and Eastoe, J., *Stimuli-responsive surfactants.* Soft Matter, 2013. **9**(8): p. 2365-2374.
7. IUPAC, *International Union of Pure and Applied Chemistry, Compendium of Chemical Terminology, Gold Book Version 2.3.3*. 2014.
8. Kronberg, B., Holmberg, K, and Lindman, B., *Surface Chemistry of Surfactants and Polymers*, 2014, Chichester, West Sussex: John Wiley & Sons.
9. Israelachvili, J., *Intermolecular and Surface Forces*, 2011, London: Academic press.
10. Holmberg, K., *Surfactants*, in *Ullmann's Encyclopedia of Industrial Chemistry,* 2019, Wiley-VCH Verlag GmbH & Co., Weinheim. p. 1-56.
11. Kawasaki, H., et al., *Reversible vesicle formation by changing pH.* Journal of Physical Chemistry B, 2002. **106**(7): p. 1524-1527.
12. Shin, J.Y. and Abbott, N.L., *Using light to control dynamic surface tensions of aqueous solutions of water soluble surfactants.* Langmuir, 1999. **15**(13): p. 4404-4410.
13. Anton, P., Heinze, J. and Laschewsky, A., *Redox-active monomeric and polymeric surfactants.* Langmuir, 1993. **9**(1): p. 77-85.
14. Brown, P., Alan Hatton, T. and Eastoe, J., *Magnetic surfactants.* Current Opinion in Colloid and Interface Science, 2015. **20**(3): p. 140-150.
15. Liu, Y., et al., *Switchable surfactants.* Science, 2006. **313**(5789): p. 958-960.
16. Yin, H., et al., *CO_2-induced reversible dispersion of graphene by a melamine derivative.* Langmuir, 2015. **31**(44): p. 12260-12267.
17. Yan, S., et al., *Preparation of CO_2-switchable graphene dispersions and their polystyrene nanocomposite latexes by direct exfoliation of graphite using hyperbranched polyethylene surfactants.* Polymer Chemistry, 2016. **7**(30): p. 4881-4890.
18. Zhang, Q., et al., *Reversibly coagulatable and redispersible polystyrene latex prepared by emulsion polymerization of styrene containing switchable amidine.* Macromolecules, 2011. **44**(16): p. 6539-6545.

19. Pinaud, J., et al., *2-(diethyl)aminoethyl methacrylate as a CO_2-switchable comonomer for the preparation of readily coagulated and redispersed polymer latexes.* ACS Macro Letters, 2012. **1**(9): p. 1103-1107.
20. Rezaee Shirin-Abadi, A., et al., *Tuning the aggregation and redispersion behavior of CO_2-switchable latexes by a combination of DMAEMA and PDMAEMA-b-PMMA as stabilizing moieties.* Polymer (United Kingdom), 2016. **106**: p. 303-312.
21. Darabi, A., et al., *Preparation of CO_2-switchable latexes using N-[3-(dimethylamino)propyl]-methacrylamide (DMAPMAm).* Journal of Polymer Science, Part A., Polymer Chemistry, 2017. **55**(6): p. 1059-1066.
22. Alshamrani, A.K., Vanderveen, J.R. and Jessop, P.G., *A guide to the selection of switchable functional groups for CO_2-switchable compounds.* Physical Chemistry Chemical Physics, 2016. **18**(28): p. 19276-19288.
23. Cunningham, M.F. and Jessop, P.G., *An introduction to the principles and fundamentals of CO_2-switchable polymers and polymer colloids.* European Polymer Journal, 2016. **76**: p. 208-215.
24. Zhang, Y., et al., *CO_2-switchable wormlike micelles.* Chemical Communications, 2013. **49**(43): p. 4902-4904.
25. Jiang, Z., et al., *Multiple Responsive Fluids Based on Vesicle to Wormlike Micelle Transitions by Single-Tailed Pyrrolidone Surfactants.* Langmuir, 2015. **31**(43): p. 11760-11768.
26. Jessop, P.G., Mercer, S.M. and Heldebrant, D.J., *CO_2 triggered switchable solvents, surfactants, and other materials.* Energy and Environmental Science, 2012. **5**(6): p. 7240-7253.
27. Ceschia, E., et al., *Switchable anionic surfactants for the remediation of oil-contaminated sand by soil washing.* RSC Advances, 2014. **4**(9): p. 4638-4645.
28. Chen, H., et al., *Reversibly pH-Switchable Anionic-Surfactant-Based Emulsions.* Journal of Surfactants and Detergents, 2017. **20**(5): p. 1115-1120.
29. Hampe, E.M. and Rudkevich, D.M., *Exploring reversible reactions between CO_2 and amines.* Tetrahedron, 2003. **59**(48): p. 9619-9625.
30. Wright, H.B. and Moore, M.B., *Reactions of Aralkyl Amines with Carbon Dioxide.* Journal of the American Chemical Society, 1948. **70**(11): p. 3865-3866.
31. Hampe, E.M. and Rudkevich, D.M., *Reversible covalent chemistry of CO_2.* Chemical Communications, 2002. **2**(14): p. 1450-1451.
32. George, M. and Weiss, R.G., *Chemically reversible organogels: Aliphatic amines as "latent" gelators with carbon dioxide [4].* Journal of the American Chemical Society, 2001. **123**(42): p. 10393-10394.
33. George, M. and Weiss, R.G., *Chemically reversible organogels via "latent" gelators. Aliphatic amines with carbon dioxide and their ammonium carbamates.* Langmuir, 2002. **18**(19): p. 7124-7135.
34. Belman, N., et al., *Reaction of Alkylamine Surfactants with Carbon Dioxide: Relevance to Nanocrystal Synthesis.* Nano Letters, 2009. **9**(5): p. 2088-2093.
35. Luo, B., Rossini, J.E. and Gladfelter, W.L., *Zinc Oxide Nanocrystals Stabilized by Alkylammonium Alkylcarbamates.* Langmuir, 2009. **25**(22): p. 13133-13141.
36. Yu, T., Cristiano, R. and Weiss, R.G., *From simple, neutral triatomic molecules to complex chemistry.* Chemical Society Reviews, 2010. **39**(5): p. 1435-1447.
37. Chiappisi, L., et al., *Catanionic surfactant systems—thermodynamic and structural conditions revisited.* Colloid and Polymer Science, 2015. **293**(11): p. 3131-3143.

38. Caplow, M., *Kinetics of carbamate formation and breakdown.* Journal of the American Chemical Society, 1968. **90**(24): p. 6795-6803.
39. Murphy, L.J., et al., *Structurally simple complexes of CO2.* Chemical Communications, 2015. **51**(19): p. 3942-3956.
40. Evans, D.F., Wennerström. H., *The Colloidal Domain where physics, chemistry, biology and technology meet*, ed. n. edition. 1999, Canada: Wiley-VCH.
41. Hamaker, H.C., *The London-van der Waals attraction between spherical particles.* Physica, 1937. **4**(10): p. 1058-1072.
42. Claesson, P.M., et al., *Short-range interactions between non-ionic surfactant layers.* Physical Chemistry Chemical Physics, 2006. **8**(47): p. 5501-5514.
43. Wall, S., *The history of electrokinetic phenomena.* Current Opinion in Colloid and Interface Science, 2010. **15**(3): p. 119-124.
44. Stern, O., *Zur Theorie der Elektrolytischen Doppelschicht.* Zeitschrift für Elektrochemie, 1924. **30**: p. 508.
45. Bijlard, A.C., et al., *Functional Colloidal Stabilization.* Advanced Materials Interfaces, 2017. **4**(1).
46. Fuhrmann, K., et al., *Modular design of redox-responsive stabilizers for nanocrystals.* ACS Nano, 2013. **7**(9): p. 8243-8250.
47. Brown, P., et al., *Magnetic emulsions with responsive surfactants.* Soft Matter, 2012. **8**(29): p. 7545-7546.
48. Nuyken, O. and Meindl, K., *A light-sensitive diazosulfonate surfactant as emulsifier for emulsion polymerization.* Journal of Macromolecular Science, Part A, 1995. **32**(4): p. 447-457.
49. McKee, J.R., et al., *Synthesis of sterically-stabilized polystyrene latexes using well-defined thermoresponsive poly(N-isopropylacrylamide) macromonomers.* Macromolecules, 2011. **44**(19): p. 7692-7703.
50. Ding, Y., et al., *Reversible dispersion of single-walled carbon nanotubes based on a CO_2-responsive dispersant.* Langmuir, 2010. **26**(22): p. 16667-16671.
51. Palme, A., *Recycling of cotton: characterization, pretreatment, and purification*. Vol. PhD. 2017, Gothenburg: Chalmers University of Technology, Sweden
52. Taylor, M.A., *Technology of Textile Properties: An introduction*, 1981. Forbes Publications Ltd.
53. Burkinshaw, S.M., *Physico-chemical Aspects of Textile Coloration*, 2016. John Wiley & Sons.
54. Stana-Kleinschek, K. and Ribitsch, V., *Electrokinetic properties of processed cellulose fibers.* Colloids and Surfaces A: Physicochemical and Engineering Aspects, 1998. **140**(1-3): p. 127-138.
55. Pearce, C.I., Lloyd, J.R and Guthrie, J.T., *The removal of colour from textile wastewater using whole bacterial cells: A review.* Dyes and Pigments, 2003. **58**(3): p. 179-196.
56. Rupin, M., *Dyeing with direct and fiber reactive dyes.* Textile Chemist and Colorist, 1976. **8**(9): p. 54-58.
57. Hauser, P.J., *Reducing pollution and energy requirements in cotton dyeing.* Textile Chemist and Colorist and American Dyestuff Reporter, 2000. **32**(6): p. 44-48.
58. Sha, F., *Studies on dyeing cationized cotton*. 2016, North Carolina: North Carolina State University, USA

59. Wang, L., et al., *Preparation of cationic cotton with two-bath pad-bake process and its application in salt-free dyeing.* Carbohydrate Polymers, 2009. **78**(3): p. 602-608.
60. Aktek, T., Millat, A.K.M.M., *Salt Free Dyeing of Cotton Fiber - A Critical Review.* International Journal of Textile Science, 2017. **6(2)**: p. 21-33.
61. Fang, K., et al., *Pigment dyeing of polyamide-epichlorohydrin cationized cotton fabrics.* Journal of Applied Polymer Science, 2010. **118**(5): p. 2736-2742.
62. Hynes, J., Novotný, T., Dr. Nič, M., *Literature study on the uses and risks of nanomaterials as pigments in the European Union* 2018, ECHA (European Chemical Agency).
63. Aspland, J.R., *Series on dyeing. Chapter 14. Pigments as textile colorants. Pigmenting or pigmentation.* Textile Chemist and Colorist, 1993. **25**(10): p. 31-37.
64. Hussain, T. and Ali, R., *Comparison of properties of cotton fabric dyed with pigment and reactive dye.* Journal of the Textile Institute, 2009. **100**(1): p. 95-98.
65. Lever, T., *Focus on cotton. Exhaust dyeing with pigments on cotton piece and garments.* Journal of the Society of Dyers and Colourists, 1992. **108**(11): p. 477-478.
66. Rojvoranun, S., et al., *Mechanistic studies of particulate soil detergency: II: Hydrophilic soil removal.* Journal of Surfactants and Detergents, 2012. **15**(6): p. 663-677.
67. Bajpai, D. and Tyagi, V.K., *Laundry detergents: an overview.* Journal of oleo science, 2007. **56**(7): p. 327-340.
68. Berry, J.D., et al., *Measurement of surface and interfacial tension using pendant drop tensiometry.* Journal of Colloid and Interface Science, 2015. **454**: p. 226-237.
69. Rosen, M.J., *Surfactants and Interfacial Phenomena,*Third Edition. 2004, Wiley & Sons, Inc., Hoboken, New Jersey.
70. Martínez-Balbuena, L., et al., *Applicability of the Gibbs Adsorption Isotherm to the analysis of experimental surface-tension data for ionic and nonionic surfactants.* Advances in Colloid and Interface Science, 2017. **247**: p. 178-184.
71. Keeler, J., *Understanding NMR Spectroscopy*. 2010, Wiley & Sons, West Sussex, United Kingdom
72. Wäsche, R., Naito, M and Hackley, V.A., *Experimental study on zeta potential and streaming potential of advanced ceramic powders.* Powder Technology, 2002. **123**(2-3): p. 275-281.
73. Corporation, B.I., *Instruction manual for ZetaPALS, Zeta Potential Analyser*. 1994, New York, USA.
74. Corporation, C., *Coulter N4 Plus Submicron Particle Sizer*. 1995: Miami, Florida, USA.
75. Sharma, G., *Digital color imaging handbook*. Digital Color Imaging Handbook. 2017. 1-797.
76. Belli Dell'Amico, D., et al., *Converting Carbon Dioxide into Carbamato Derivatives.* Chemical Reviews, 2003. **103**(10): p. 3857-3897.
77. Carroll, J.J., Slupsky, J.D. and Mather, A.E., *The Solubility of Carbon Dioxide in Water at Low Pressure.* Journal of Physical and Chemical Reference Data, 1991. **20**(6): p. 1201-1209.

78. McCann, N., et al., *Kinetics and mechanism of carbamate formation from CO_2(aq), carbonate species, and monoethanolamine in aqueous solution.* Journal of Physical Chemistry A, 2009. **113**(17): p. 5022-5029.
79. Bordes, R., Tropsch, J. and Holmberg, K., *Role of an amide bond for self-assembly of surfactants.* Langmuir, 2010. **26**(5): p. 3077-3083.
80. Oskarsson, H., et al., *Adsorption of novel alkylaminoamide sugar surfactants at tailor-made surfaces.* Journal of Surfactants and Detergents, 2007. **10**(1): p. 41-52.
81. Burns, N.L., Holmberg, K. and Brink, C., *Influence of surface charge on protein adsorption at an amphoteric surface: Effects of varying acid to base ratio.* Journal of Colloid and Interface Science, 1996. **178**(1): p. 116-122.
82. *Trends in atmospheric Carbon Dioxide*. 2019 [cited 2019 October 7th, 2019].
83. Kanicky, J.R. and Shah, D.O., *Effect of premicellar aggregation on the pKa of fatty acid soap solutions.* Langmuir, 2003. **19**(6): p. 2034-2038.
84. Tsubone, K., Arakawa, Y and Rosen, M.J., *Structural effects on surface and micellar properties of alkanediyl- α,ω -bis(sodium N -acyl- β -alaninate) gemini surfactants.* Journal of Colloid and Interface Science, 2003. **262**(2): p. 516-524.
85. Zana, R., *Dimeric and oligomeric surfactants. Behavior at interfaces and in aqueous solution: A review.* Advances in Colloid and Interface Science, 2002. **97**(1-3): p. 205-253.
86. Bordes, R., Tropsch, J. and Holmberg, K., *Counterion specificity of surfactants based on dicarboxylic amino acids.* Journal of Colloid and Interface Science, 2009. **338**(2): p. 529-536.
87. Li, Z.X., Dong, C.C. and Thomas, R.K., *Neutron reflectivity studies of the surface excess of gemini surfactants at the air-water interface.* Langmuir, 1999. **15**(13): p. 4392-4396.
88. Wüstneck, N., et al., *On the dissolution of vapors and gases.* Langmuir, 2007. **23**(4): p. 1815-1823.
89. Thompson, D.W., *Effect of interfacial mobility on mass transfer in gas-liquid systems.* Ind Eng Chem Fundam, 1970. **9**(2): p. 243-248.
90. Llorens, J., Mans, C. and Costa, J., *Discrimination of the effects of surfactants in gas absorption.* Chemical Engineering Science, 1988. **43**(3): p. 443-450.
91. Yang, J. and Dong, H., *CO_2-responsive aliphatic tertiary amine-modified alginate and its application as a switchable surfactant.* Carbohydrate Polymers, 2016. **153**: p. 1-6.
92. Su, X., et al., *A conventional surfactant becomes CO_2-responsive in the presence of switchable water additives.* Chemistry - A European Journal, 2013. **19**(18): p. 5595-5601.
93. Hao, L., et al., *Investigating the adsorption performance of nanoscale pigment on cationized cotton substrate.* Powder Technology, 2012. **222**: p. 176-181.
94. Shateri Khalil-Abad, M., Yazdanshenas, M.E and Nateghi, M.R., *Effect of cationization on adsorption of silver nanoparticles on cotton surfaces and its antibacterial activity.* Cellulose, 2009. **16**(6): p. 1147-1157.
95. Montazer, M., Malek, R.M.A. and Rahimi, A., *Salt free reactive dyeing of cationized cotton.* Fibers and Polymers, 2007. **8**(6): p. 608-612.
96. Hauser, P.J. and Tabba, A.H., *Improving the environmental and economic aspects of cotton dyeing using a cationised cotton.* Coloration Technology, 2001. **117**(5): p. 282-288.

97. Fang, K., et al., *Dyeing of cationised cotton using nanoscale pigment dispersions.* Coloration Technology, 2005. **121**(6): p. 325-328.
98. Sandberg, R.G., et al., *Kinetics of acid dissociation-ion recombination of aqueous methyl orange.* The Journal of Physical Chemistry, 1972. **76**(26): p. 4023-4025.
99. Hong, K.H., *Preparation and properties of multi-functional cotton fabric treated by gallnut extract.* Textile Research Journal, 2014. **84**(11): p. 1138-1146.
100. Tiwari, A., Jain, R., *Effect of mercerization under tension on the drapability and strength of cotton khadi fabric.* International Journal of Research in Applied, Natural and Social Sciences, 2017. **5**(4): p. 19-26.